Ecological Modelling 516 (2026) 111578

Contents lists available at ScienceDirect

Ecological Modelling

journal homepage: www.elsevier.com/locate/ecolmodel

From calibration to identifiability analysis: Using a multi-reserve DEB model to understand holopelagic *Sargassum* spp. growth☆

María-José Lagunes [a,b,*], Gonçalo M. Marques [c], Evelyn R. Salas-Acosta [d,e], Roman M. Vásquez-Elizondo [e], Thierry Thibaut [d], Daniel Robledo [e], Solène Connan [b], Valérie Stiger-Pouvreau [b], Léo Berline [d], Christophe Lett [a], Laure Pecquerie [b,f,**]

[a] MARBEC, IRD, Univ Montpellier, CNRS, Ifremer, Sète, 34200, France
[b] Univ Brest, IRD, CNRS, Ifremer, LEMAR, IUEM, Plouzané, F-29280, France
[c] MARETEC/LARSyS, Instituto Superior Técnico, Universidade de Lisboa, 1049-001, Lisboa, Portugal
[d] Aix Marseille Univ, Université de Toulon, CNRS, IRD, MIO, Marseille, 13228, France
[e] Cinvestav, Merida Unit, Department of Marine Resources, Carretera Antigua a Progreso, A.P. 73 Cordemex, Mérida, 97310, Yucatán, Mexico
[f] ISI, Computer Science Department, FSSM, Cadi Ayyad University, Bd. Prince My Abdellah, 40000 Marrakesh, Morocco

ARTICLE INFO

Dataset link: SargaDEB_SFF_NeededExperiments (Original data)

Keywords:
Parameter estimation
Bioenergetics
Macroalgae
Virtual ecologist approach
Experimental design

ABSTRACT

Unprecedented quantities of the brown floating macroalgae *Sargassum* have been recorded in the tropical North Atlantic Ocean. However, the environmental factors affecting holopelagic *Sargassum* spp. growth and survival remain poorly understood. Here, we developed a multi-reserve DEB model for *Sargassum* spp. to link environmental conditions (temperature, nutrients, and light) to the organism physiology. In the context of DEB theory, estimating a multi-reserve model parameters can be particularly challenging and strongly relies on the availability of the datasets with information about physiological processes. We conducted a literature review of *Sargassum* spp. physiological responses, and although some data have been reported, experimental datasets on some key physiological processes are still relatively scarce. From the available data we performed an estimation of the DEB model parameters. We then followed a "virtual ecologist" approach to create a framework linking modelers and empiricists, to analyze which experiments that are most needed to reduce parameter uncertainty. We tested parameter identifiability by creating *"virtual" observed data* and we analyzed the type of datasets that reduce the uncertainty on parameter estimates, thus increasing their identifiability and the prediction power of the algae model. Our analysis showed to which extent new experiments on nutrient uptake and nutrient limitation would reduce the uncertainty of key model parameters and improve our understanding of holopelagic *Sargassum* spp. physiology. More generally, our study demonstrates how the use of DEB models, coupled with parameter identifiability analyses, can help design most needed experiments thereby contributing to an integrated approach between experiments and modeling.

1. Introduction

Macroalgal blooms are a growing concern impacting marine ecosystems, society, and economic entities (Sellner et al., 2003). Recently, one of the most notable macroalgal blooms involves the holopelagic *Sargassum* spp. in the tropical Atlantic Ocean. These brown macroalgae were initially located within the North Atlantic gyre in a zone called the *Sargasso* sea. However, since 2011, the distribution of these macroalgae has expanded to the tropical Atlantic and the Caribbean, where they found favorable conditions to grow, creating what is now called the Great Atlantic *Sargassum* Belt (GASB) (Wang et al., 2019). This new accumulation of biomass along with the Atlantic circulation causes massive strandings of holopelagic *Sargassum* spp. along the coasts of the Gulf of Mexico, Antilles, Central America, Brazil, and tropical Africa, having social, economic, health, and ecological impacts on coastal communities (Schell et al., 2015; Wang et al., 2019; Fidai et al., 2020).

Modeling efforts to understand holopelagic *Sargassum* spp. influx have focused mainly on the transport and physical drivers for the observed spatio-temporal variability (Berline et al., 2020; Putman et al.,

☆ This article is part of a Special issue entitled: 'DEB2025' published in Ecological Modelling.

* Corresponding author at: MARBEC, IRD, Univ Montpellier, CNRS, Ifremer, Sète, 34200, France.
** Correspondence to: ISI, Computer Science Department, FSSM, Cadi Ayyad University, Bd. Prince My Abdellah, 40000 Marrakesh, Morocco.
E-mail addresses: maria_jose.lagunes@ird.fr (M.-J. Lagunes), laure.pecquerie@ird.fr (L. Pecquerie).

https://doi.org/10.1016/j.ecolmodel.2026.111578
Received 18 November 2025; Received in revised form 17 March 2026; Accepted 21 March 2026
Available online 26 March 2026

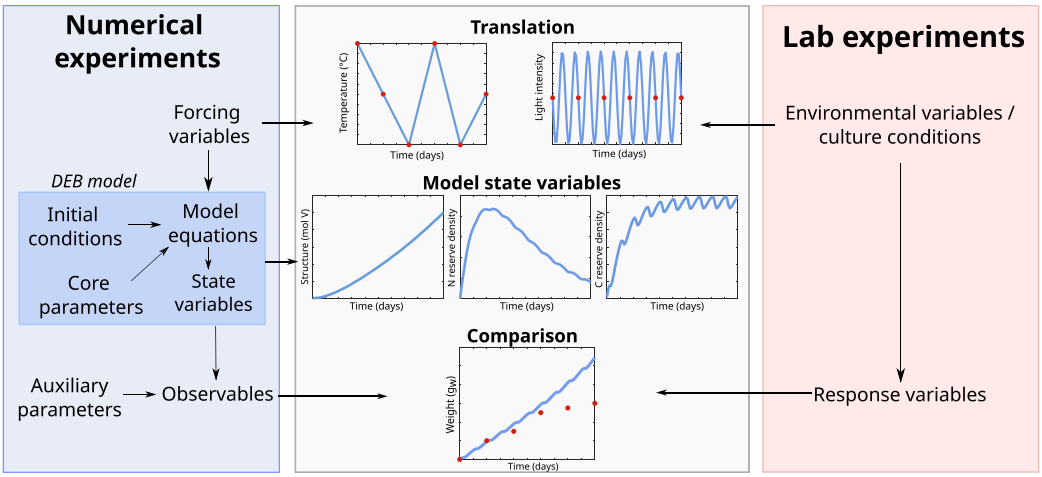

Fig. 1. Correspondence between laboratory experiments (observations, red dots) and numerical experiments (simulations, blue lines). The grey, central panel illustrates the correspondence between model forcing variables and environmental variables (top line), DEB model resulting state variables (medium line) and the correspondence between model observables and response variables obtained in the lab (bottom line). Adapted from Kearney et al. (2021) and Lika et al. (2011).

2020; Marsh et al., 2021). Comparatively, few models have incorporated holopelagic *Sargassum* spp. biology, which is critical to estimate the biomass of these species (Brooks et al., 2018; Jouanno et al., 2021; Marsh et al., 2022; Payne et al., 2024). Furthermore, the limited knowledge on the physiological responses to temperature and nutrient availability hinders the understanding of the inter-annual variability of holopelagic *Sargassum* spp. biomass across different regions. To contribute to filling this gap, we propose a mechanistic model of holopelagic *Sargassum* spp. growth based on Dynamic Energy Budget (DEB) theory.

DEB models are based on the principles of mass conservation and thermodynamics, allowing the study of the allocation of energy to different physiological mechanisms according to the environmental conditions encountered (Kooijman, 2010). In the case of an autotrophic organism, such as holopelagic *Sargassum* spp. this is possible by using a multi reserve DEB model, that allows to dynamically quantify the use of light and assimilation of nutrients to produce biomass, maintain the organisms metabolism and survive (Kooijman, 2010). Nonetheless, a limited number of multi-reserve DEB models have been developed for microalgae (Lika and Papadakis, 2009; Lorena et al., 2010; Livanou et al., 2019) and for green (*Ulva lactuca*, Lavaud et al. (2020)) and brown (*Saccharina latissima*, Venolia et al. (2020)) macroalgae, but there is none for holopelagic *Sargassum* spp.

A mechanistic bioenergetic model is an abstract representation of an organism that uses a set of equations, parameters, and inputs such as environmental conditions to describe a studied system (Meer, 2006). Using such models allows us to compare the organism's responses (or observables) to environmental conditions with the outputs predicted by the model (Fig. 1, Appendix C). However, this also means that species-specific parameters must be estimated if we want to understand a given species, which requires data collected under different environmental conditions to obtain reliable parameter estimates (Marques et al., 2019).

In ecological modeling, data availability is often limited due to the cost and time required for experimental work, which can make it difficult to allow a good fit between model predictions and observed data, while maintaining biologically realistic parameters (Marques et al., 2019; Lika and Kooijman, 2024). Additionally, when dealing with complex models and a limited amount of data, different sets of parameters can explain the same data, leading to a problem of parameter identifiability (Wieland et al., 2021; Lam et al., 2022). In the case of holopelagic *Sargassum* spp., since 2011, studies have mainly focused on the effect of temperature on growth rate, however, few have focused on differences according to nutrient availability (Magaña-Gallegos et al., 2023b,a; Schell et al., 2024; Corbin and Oxenford, 2023; Changeux et al., 2023; Hatt et al., 2025). To overcome this issue, we adopt a Virtual Ecologist Approach (VEA) (Zurell et al., 2010) to assess parameter identifiability in the DEB framework, with the objective of providing a protocol for interaction between modelers and empiricist aimed at identifying optimal experimental designs (Raue et al., 2010; Guillaume et al., 2019). This approach relies on mimicking an experimental design and virtual datasets by using known 'true' parameter values. These virtual model outputs are treated as error-free observations that are then used to estimate parameters and evaluate whether these known 'true' parameters can be retrieved. In this way, when the "true" parameters are not retrieved, the information contained in the datasets is not enough to constrain the parameters. This approach follows the principle of practical identifiability analysis (Guillaume et al., 2019) and represents an implementation of VEA focused on parameter estimation. By placing the modeler in the place of empiricist, this framework allows the evaluation of the experimental design and facilitates the interaction with empiricists (Jakeman et al., 2024).

The objectives of this study were twofold: first, to develop a model for studying the physiology of holopelagic *Sargassum* spp. and second, to identify data that could improve the estimation of the model parameters. To do so, we developed a multi-reserve DEB model to study the effect of nutrient uptake, light intensity, and temperature on holopelagic *Sargassum* spp. growth. Then, we described the different available data, the selection of the datasets and the estimation of the model parameters. Finally, by using a methodology for parameter identification and the use of a "virtual ecologist" approach, we generated "virtual" experimental data using our DEB model and assessed to which extent these different experimental datasets would reduce the uncertainty of the parameter estimates. This broad approach provides a protocol for evaluating the contribution of experiments to understand holopelagic *Sargassum* spp. growth.

2. Material and methods

2.1. Multi-reserve DEB model description

The multi-reserve DEB theory provides a conceptual and quantitative framework to study the effect of environmental conditions on *Sargassum* spp. physiology. Based on the DEB model studies for microalgae and macroalgae developed by Lorena et al. (2010), Venolia et al. (2020) and Lavaud et al. (2020), we implemented the multi-reserve equations for holopelagic *Sargassum* spp., considering the following set of assumptions. We considered that each state variable has a constant

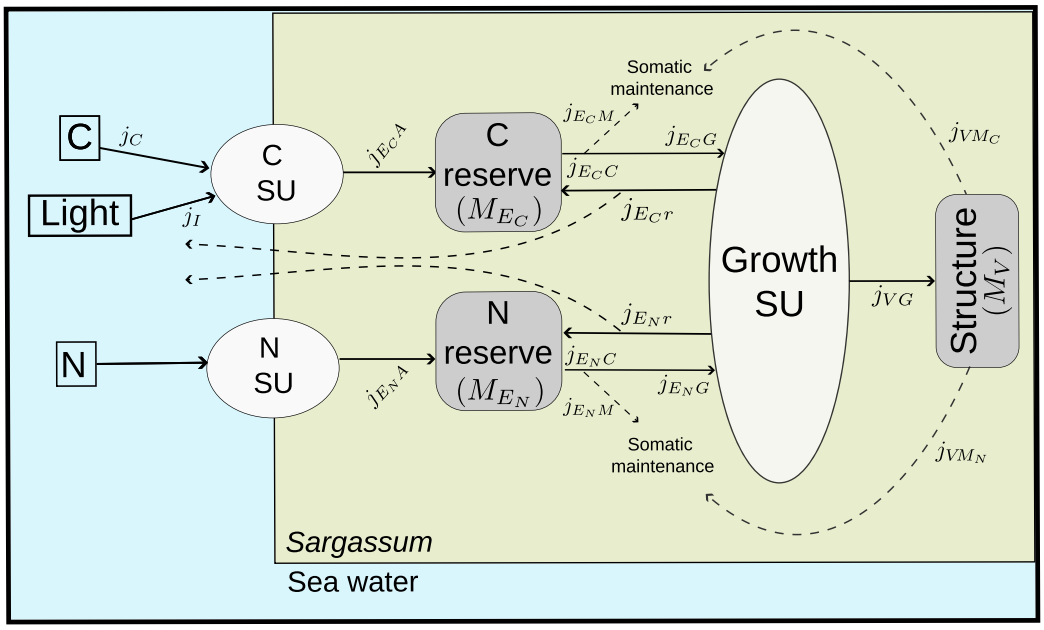

Fig. 2. Schematic representation of the multi-reserve model for holopelagic *Sargassum* spp. Rectangles outside the sargassum cell represent the forcing variables (carbon [C], light, and nitrogen [N]). Temperature is not represented explicitly for simplicity's sake, but all fluxes are impacted by temperature following the Arrhenius formulation described in Appendix B. White circles within the cell represent synthesizing units (SUs) where transformations occur. Grey rectangles denote the model state variables. Solid arrows represent fluxes within the organism, while dashed arrows indicate fluxes released to the environment through excretion or via maintenance costs paid by each reserve or by the structure. All abbreviations can be found in Appendix A and in Kooijman (2010).

Table 1
State variables and forcing variables of the multi-reserve DEB model.

Variables	Notation	Unit
N reserve	M_{E_N}	mol M_{E_N}
C reserve	M_{E_C}	mol M_{E_C}
Structure	M_V	mol M_V
Temperature	T	°C (K for simulations)
[Nitrogen]	[N]	mol N L^{-1}
[Inorganic carbon]	[C]	mol CO_2 L^{-1}
Light	I	mol E cm^{-2} h^{-1}

chemical composition (strong homeostasis), which allows us to perform the mass balance at each time step to study resource allocation for different physiological processes (Sousa et al., 2010). Additionally, assimilation processes are proportional to surface area and maintenance processes to volume. Also, because no sexual reproductive structures or receptacles have ever been observed on holopelagic *Sargassum* spp. thalli, and it is thus assumed that these sargassum reproduce only by fragmentation (Siuda et al., 2024), sexual reproduction was not considered in this model. Because of this and since organisms of holopelagic *Sargassum* spp. have been observed to grow primarily along the *y*-axis, it is assumed that the organisms behave as V1-morphs, which means that surface area is proportional to volume (Kooijman, 2010; Chambon, 2022). This will ultimately simplify model equations and make them transposable to a population model. Finally, in order to establish a mechanistic uptake formulation for each reserve, the multi-reserve model relies on the concept of *synthesizing units* (SUs), which can be described as enzymes or enzyme complexes that bind a substrate molecule to deliver a product molecule or a set of product molecules based on the arrival flux of each substrate instead of the substrate concentration (Kooijman, 1998, 2010; Poggiale et al., 2010). Model state variables and forcing conditions can be found in Table 1.

The multi-reserve model dynamics are described as follows (Fig. 2, Appendix A): nutrients are transformed and assimilated into reserves by an assimilation SU. Each reserve is then mobilized and allocated with priority to maintenance, and the remaining portion is allocated to a growth SU. The reserve represents biomass that does not require maintenance and is used as a source of energy or building blocks (Jusup et al., 2017). In this study, we focused on carbon and nitrogen reserves (C and N) to capture physiological dynamics; an additional phosphorus reserve could be incorporated within the DEB framework (Grossowicz et al., 2017) and will be considered in future development. Maintenance is described as the set of physiological processes an organism needs to continue living (e.g. maintenance of concentration gradients across membranes, and protein turnover) (Lorena et al., 2010; Kooijman, 2010). In the case of the growth SU, substrates are transformed to produce structure. The structure represents biomass that needs to be maintained, with the total biomass of an organism being the sum of all reserves and structure. The growth SU follows a complementary parallel SU (Section 3.7.3 Kooijman, 2010; Poggiale et al., 2010), meaning that both substrates are necessary to produce structure. If there is an excess of one substrate, or if there is insufficient quantity of one substrate for the growth SU to process both substrates at the same time, the non-limiting substrate cannot be processed until the required quantity of the limiting substrate is available. Because the binding sites of the growth SU are already occupied by the non-limiting substrate, additional substrate is rejected, and it is either reincorporated into its reserve or excreted into the environment. Finally, when the reserve content is not sufficient to pay for maintenance costs, organisms will break down structure to meet the remaining requirements. As a preliminary evaluation, we tested our multi-reserve DEB model and confirmed that it could reproduce the general patterns observed for holopelagic *Sargassum* spp. (Table 2, Supplementary material, Figure S1).

2.2. Experimental data available for holopelagic Sargassum spp.

To build a set of parameters more specific to holopelagic *Sargassum* spp., we conducted a literature review using Google Scholar to identify *in-situ* or *ex-situ* experimental studies involving the collection of any of the three recognized morphotypes of holopelagic *Sargassum* spp., and reporting at least one measurement of a response variable.

To integrate the data from the literature review into the DEB multi-reserve model, we translated the lab experiments variables (the experimental protocol and response variables) into the numerical experiments variables (the model inputs and outputs) (Fig. 1). Lab experiments variables are the culture conditions (or *in-situ* conditions), initial conditions, experiment duration, measurements and the associated response variables reported. In numerical experiments, this translates respectively to the forcing variables, initial conditions of the state variables, the duration of the simulation, the evolution of state variables during simulation and the observables. From each literature study, we also gathered the morphotype studied, the location of collection, and the type of culture (*in-situ* or *ex-situ*).

From all available datasets we selected those with the most comprehensive experimental data describing *ex-situ* experiments (See Supplementary material). We focused on the completeness of forcing variables, the collection site (tropical Atlantic), and the description of initial conditions. However, when datasets were missing information, we inferred missing values from similar experimental conditions or typical conditions at sea. For example, in the case of inorganic carbon, values were inferred as the mean value for the tropical Atlantic Ocean.

In the following sections, although data were compiled for all three holopelagic morphotypes (See Supplementary material), only observations of *S. fluitans* var. *fluitans* were used for analysis, simulations and parameter estimation, as this is the morphotype with the largest amount of data (Changeux et al., 2023; Corbin and Oxenford, 2023).

2.3. Estimation of *Sargassum fluitans var. fluitans*DEB parameters

Description of AmP procedure. DEB parameter estimation is performed using the dedicated AmP procedure (Marques et al., 2018), based on well-defined and species-specific codes available in the DEB collection (AmPspeciescollection). As there were no AmP codes available for *Sargassum* spp., we first had to adapt the user-defined animal codes to create functions for the species. These files can be found in the Supplementary material, as well as a description of the required files.

In this framework, the DEBtool_M package is used to estimate parameter values through an automated optimization procedure. The objective of the parameter estimation algorithm is to minimize the deviation between observations from experimental studies or field datasets and the corresponding model predictions across all available datasets (Lika et al., 2011). To do this, the algorithm uses a symmetric bounded loss function, which accounts for differences in units among datasets and a relative weight given to datasets (Marques et al., 2018). Model predictions are generated for a given parameter set, the loss function is computed, and parameters are iteratively evaluated using the Nelder–Mead simplex method until convergence is reached or a user-defined maximum number of iterations is exceeded.

AmP procedure implementation. Using the AmP procedure described above and the available datasets selected we proceeded with the estimation of parameters (Fig. 3, Step 1). Parameter estimation needs an initial set of parameter values. As DEB parameters have not been estimated for *Sargassum fluitans* var. *fluitans*, the parameters of a closely-related species are used as initial values. Here, parameters were retrieved from Venolia et al. (2020), which modeled the growth and survival of the brown macroalga *Saccharina latissima* (See Supplementary material).

First, we estimated the temperature related parameters (T_A, T_H, T_L, T_{AH}, and T_{AL}) to reflect the response to the temperatures experienced by holopelagic *Sargassum* spp. along their trajectory in the tropical Atlantic. To perform the estimation, we used the existing data on growth rates of *Sargassum fluitans* var. *fluitans*. As no data below 21 °C was available, growth rates of *S. natans* var. *natans* from Hanisak and Samuel (1987) were used as supplementary information (See Supplementary material for the detailed explanation of this step).

Then we estimated the selected model parameters, using the available datasets. For each dataset, the initial values for the C and N reserves densities were set up as m_{E_C0} = 0.002 mol C mol V^{-1} and m_{E_N0} = 0.01 mol N mol V^{-1} respectively (Venolia et al., 2020). The initial value for the structure (M_{V_0}) was obtained for each dataset by converting the initial condition of the algae (e.g. wet weight) at the beginning of an experiment into structure using the model parameters and the initial values of the corresponding reserve densities (Appendix C).

2.4. Identifiability analysis and protocol to guide experimental design

Following the virtual ecologist approach described by Zurell et al. (2010), we analyzed parameter identifiability to design experiments that would reduce parameter uncertainty (Raue et al., 2010)(Fig. 3, Step 2). In this approach, (i) an ecological model, in this case the multi-reserve DEB model, (ii) a virtual organism characterized by *"true" parameters* and (iii) simulations which are mimicking experiment designs, are used to generate *"virtual" observed data*. From these *"virtual" observed data*, parameters are estimated and subsequently evaluated against the *"true" parameters* used for the simulation. This framework allows for the assessment of the available datasets and the identification of new experimental designs that could improve parameter identifiability.

Following this protocol, we evaluated whether the available data are sufficient to estimate the selected model parameters (Fig. 3) (Raue et al., 2010). For this, we defined a set of "true" parameters corresponding to the resulting estimated values of the previous section. Using these parameters, we conducted numerical experiments that mimicked the available lab experiments detailed in Section 2.2, reproducing both the forcing conditions and response variables measured. The resulting datasets are referred as *selected "virtual" observed data*.

In addition to these datasets, we generated datasets which were not available for *Sargassum* spp. in order to evaluate whether such data could provide valuable information on *Sargassum* spp. physiology and reduce model parameter uncertainty. This datasets are generated using the multi-reserve DEB model and the "true" parameters. We refer to these datasets as *new "virtual" observed data*. Because all *"virtual" observed data* are generated using the model and derived from known "true" parameters, we can directly assess if a given type of data allows to retrieve the *"true" parameters*. This allows to identify optimal laboratory experiments that enhance parameter identifiability (Guillaume et al., 2019).

The *new "virtual" observed data* were designed based on: (i) missing data types by comparing our datasets with those used to calibrate the other DEB algae models (Grossowicz et al., 2017; Lavaud et al., 2020; Venolia et al., 2020) and (ii) missing information on *Sargassum* spp. physiology. First, we created *new "virtual" observed data* of nutrient uptake for different nitrate (NO_3^-) concentrations at different temperatures. Then, a starvation *new "virtual" observed data* was created by setting lower total nutrient concentrations and irradiance to simulate nutrient limitation. The forcing conditions and initial conditions corresponding to the *new "virtual" experiments* producing these *new "virtual" observed data* can be found in the Supplementary material, together with the codes used to generate these *"virtual" observed data*.

To quantify the effect of each *available* experimental dataset and of the proposed *new "virtual" observed data* on parameter estimates, we generated new sets of initial parameter values by simultaneously deviating a selection of the *"true" parameters* by ± 10%. The selected parameters were estimated, while the remaining parameters were kept fixed at their reference values. The choice of parameters was guided by the type of data missing on the physiology of holopelagic *Sargassum* spp. and which we consider will provide more information on the species physiology.

Once this set, we proceeded with the parameter estimation by testing different combinations of *available* and *new "virtual" observed data* to evaluate how specific datasets contribute to parameter identifiability. For all estimations, the weight assigned to each dataset was set to 1, so

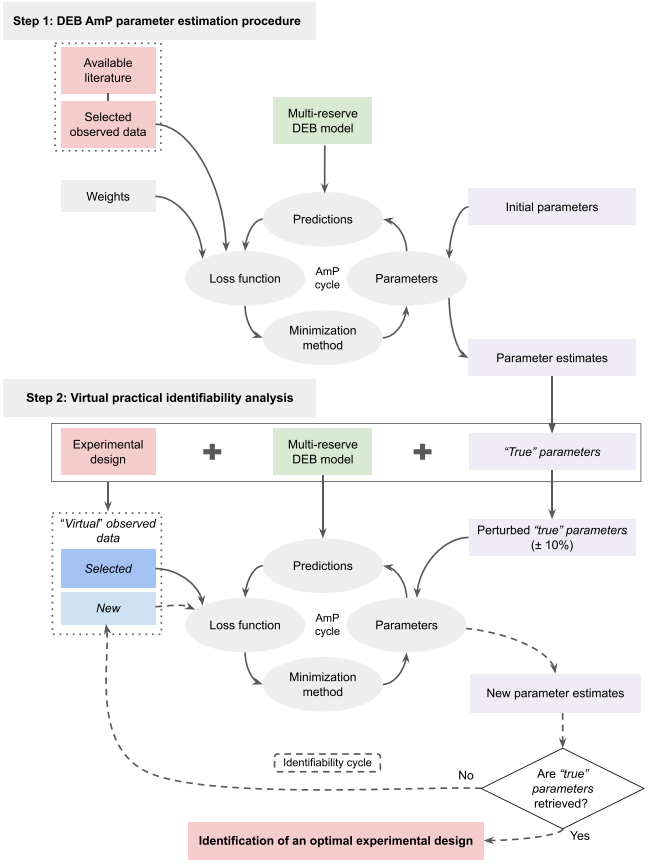

Fig. 3. Approach for parameter estimation and virtual practical identifiability analysis to identify an optimal experimental design (Modified from Marques et al. (2018) and Zurell et al. (2010)). Step 1 consists of selecting observed data from literature (dotted box, see Section 3), and applying the AmP cycle to estimate model parameters (Marques et al., 2018). These parameter estimates are then used in Step 2, which describes the protocol for (i) generating "virtual" observed data (Zurell et al., 2010), and (ii) evaluating if these data improved parameter identifiability. *Selected "virtual" observed data* are generated from existing datasets, and additional *new "virtual" observed data* (dashed lines) are iteratively added (dashed lines) to test whether new types of data improves parameter identifiability. Blue boxes represent numerical experiments (model-generated data), with two shades differentiating between the two types of *"virtual" observed data*. Red boxes represent data or information related to laboratory experiments. Grey ovals represent the AmP estimation procedure, the green box represents the multi-reserve DEB model developed in this study, and light purple boxes indicate the different parameter sets used and obtained during the procedure.

that all datasets contributed equally to the estimation process (Marques et al., 2018).

Precisely, the tested combinations of *selected* and *new "virtual" observed data*, later referred to as Simu *i*, were:

- Simu 1: all *selected "virtual" observed data* except the photosynthesis dataset
- Simu 2: all *selected "virtual" observed data*
- Simu 3: all *selected "virtual" observed data* + the nutrient uptake *new "virtual" observed data*
- Simu 4: all *selected "virtual" observed data* + the starvation *new "virtual" observed data*
- Simu 5: all *selected "virtual" observed data* except the photosynthesis dataset + all *new "virtual" observed data*,
- Simu 6: all *available* and *new "virtual" observed data*

For each parameter (θ) and each simulation, we calculated the symmetric squared error (SSE, Eq. (1)) between the *"true"* value (θ_{true}) and the estimated value (θ_{new}) (Accolla et al., 2020). The SSE was therefore calculated twice for each parameter, once for the positive deviations and once for the negative deviation, with all selected parameters receiving the same increment simultaneously.

$$SSE_\theta = sign(\theta_{new} - \theta_{true}) \frac{(\theta_{new} - \theta_{true})^2}{\theta_{new}^2 + \theta_{true}^2} \quad (1)$$

Finally, for each parameter, SSE values resulting from the positive and negative perturbation were evaluated independently across all datasets combinations. This comparison allowed us to quantify how the inclusion of specific datasets reduced estimation error and improved parameter identifiability. Therefore, this protocol enabled us to identify the type of observations that provide the most informative data for parameter estimation (Raue et al., 2010).

Table 2
Summary of experimental data conducted on holopelagic *Sargassum* spp. The abbreviations correspond to the morphotypes: SN *Sargassum natans*, SFF *S. fluitans* var. *fluitans*, SNN *S. natans* var. *natans*, and SNW: *S. natans* var. *wingei*.

Reference	Morphotype	Response variable
Lapointe (1986)	SFF and SN	Growth rate under nutrient enrichment conditions
Hanisak and Samuel (1987)	SNN	Growth rate as a function of temperature, salinity, and light intensity
Changeux et al. (2023)	SFF, SNN, SNW	Growth rate and nutrient content
Corbin and Oxenford (2023)	SFF, SNN, SNW	Growth rate as a function of temperature (cool vs. warm periods)
Magaña-Gallegos et al. (2023a)	SFF and SNW	*In-situ*: growth rate and nutrient content under nutrient enrichment; *Ex-situ*: growth rate at different temperatures
Magaña-Gallegos et al. (2023b)	SFF, SNN, SNW	Growth rate at different temperatures
Vásquez-Elizondo et al. (2023)	SFF and SNN	Photosynthetic rate of light-acclimated organisms, nutrient content, and growth rate
Schell et al. (2024)	SFF, SNN, SNW	Growth rate at different temperatures and salinity

3. Results

3.1. Holopelagic *Sargassum* spp. experimental data review and selected datasets

The full analysis of the reviewed experimental data conducted on holopelagic *Sargassum* spp. can be found in the Supplementary material and is summarized in Table 2. When we selected the experimental studies for this analysis (Sept. 2024), we found eight experimental studies focusing on at least one of the three holopelagic morphotypes in either the North Atlantic or the tropical Atlantic. Of these, two were conducted in the late 1980s, and six were published very recently (2023 and 2024). Most studies focused on the effect of temperature and nutrients availability on algal growth. Two studies highlighted the light-photosynthesis relationship. Most studies included at least two of the most common holopelagic forms found in the Atlantic Ocean (*Sargassum natans* var. *natans* and *Sargassum fluitans* var. *fluitans*).

There is currently no consensus on the optimal temperature for holopelagic *Sargassum* spp. growth. In particular for *Sargassum fluitans* var. *fluitans*, studies reported different trends: negative linear relationship between temperature and growth rate (Corbin and Oxenford, 2023; Magaña-Gallegos et al., 2023a), whereas others described a positive bell-shaped response (Hanisak and Samuel, 1987; Magaña-Gallegos et al., 2023b), and others a negative bell-shaped response (Schell et al., 2024). Magaña-Gallegos et al. (2023a) showed that adding nutrients *in-situ* increased the tissue N content and reduced de C:N ratios, but that growth rate was eventually reduced at a higher nutrient concentration for. Vásquez-Elizondo et al. (2023) measured the photosynthesis-irradiance (PI) curve according to acclimation, showing a hyperbolic response curve as light increased. For *S. fluitans* var.

Table 3
Datasets of *S. fluitans* var. *fluitans* used for parameter estimation. A label is given to each dataset to improve readability. HS1987: (Hanisak and Samuel, 1987); MG2023a: (Magaña-Gallegos et al., 2023a); MG2023b (Magaña-Gallegos et al., 2023b); VE2023: (Vásquez-Elizondo et al., 2023); and LP2021: (Lapointe et al., 2021).

Label	Type of data	Values
HS1987	Growth rates at 12, 18, 24, 30 °C in doublings day^{-1}	*In graphs*
MG2023a	Wet weight evolution at 28 °C and 31 °C in g_w	*In graphs*
MG2023b	Growth rates at 22, 25, 28, and 31 °C in doublings day^{-1}	*In graphs*
VE2024	Photosynthesis rates under increasing light intensities (high-light acclimated) μ mol O_2 cm^{-2} h^{-1}	*In graphs*
LP2021	Mean tissue C:N:P ratios	C:N = 32.4 C:P = 886 N:P = 27.8

fluitans they found saturating irradiance at the same level when algae were acclimated to low and high light, but with differences as for the photoinhibition and photo-acclimation effect.

For the estimation procedure, we selected data on *Sargassum fluitans* var. *fluitans* individuals collected in the tropical Atlantic Ocean and with at least one of the environmental factors controlled (Table 3 and Supplementary material). To these data we added information on the dry to wet weight ratio (*pers. comm.* and the proportion of ash and moisture on dry weight (Machado et al., 2022; Tonon et al., 2022), which resulted in the auxiliary parameters to transform dry weight into ash-free dry weight (Table 4, Appendix C).

3.2. Analysis of DEB parameter estimates

For the estimation of the temperature related parameters we used Hanisak and Samuel (1987), Magaña-Gallegos et al. (2023a), and Magaña-Gallegos et al. (2023b) datasets. The maximum growth rate was found at 28 °C, with a lower boundary at 15 °C and a upper boundary of 31 °C (Fig. 4). This indicates that the organism is growing below and above these temperatures, respectively. Finally, the decrease in growth rate above 28 °C is abrupt compared to the effect below this temperature.

Then, the remaining parameters of *Sargassum fluitans* var. *fluitans* (Table 4) were estimated using four datasets: Hatt et al. (2024), Magaña-Gallegos et al. (2023a,b), Vásquez-Elizondo et al. (2023). The resulting estimation error was of MRE = 0.026. Compared to Magaña-Gallegos et al. (2023a) dataset, we found that the prediction of the evolution of wet weight over time is consistent with the observations (Fig. 5A). However, the faster growth rate is at 28 °C in the model prediction as opposed to 31 °C in the data. Compared to Magaña-Gallegos et al. (2023b) dataset, the faster predicted growth rate was at 28 °C, like in the observations, and the slowest at 22 °C instead of 31 °C in the data (Fig. 5B). In the case of Hanisak and Samuel (1987) data, the slow growth at 12 °C was well reproduced, but we obtained the fastest growth prediction at 30 °C instead of 24 °C observed in the data (Fig. 5C). For the photosynthesis rate, the model captured well the photosynthetic capacity of the algae at 23 °C (Fig. 5D).

3.3. Identifiability analysis

The *selected "virtual" observed data* and the *new "virtual" observed data* used in the identifiability analysis are shown in Fig. 6. The resulting DEB state variables for the starvation experiment can be found in the Supplementary material section (Figure S3).

Regarding parameter identifiability of parameters across datasets (Fig. 7), adding *"virtual" observed data* on nutrient uptake reduced the estimation error of $j_{E_N Am}$ and K_N (Simu 3, 5, and 6). When photosynthesis data were excluded (Simu 1 and Simu 5), the photosynthesis parameters (ϵ_I and $\dot{k}_I$) showed higher errors compared with the simulations that included this *"virtual" observed data*. Adding starvation *"virtual" observed data*, improved the identifiability the nitrogen reserve turnover parameter ($\dot{k}_{E_N}$), although the effect of nutrient uptake data alone on this parameter is unclear as the combination of starvation and nutrient uptake data did not improve the parameter estimates (Simu 3 and 6). As for $\dot{k}_{E_C}$, this parameter is better constrained when adding both starvation and nutrient uptake *"virtual" observed data*. Starvation *"virtual" observed data* also reduced the error for the nitrogen somatic maintenance parameter $j_{E_N M}$, especially when combining it with the N uptake data (Simu 4 and 6). In contrast, the carbon somatic maintenance $j_{E_C M}$ parameter resulted in a lower error when the starvation dataset is combined with the nutrient uptake *"virtual" observed data* (Simu 6). However, adding the starvation *"virtual" observed data* alone (Simu 4) was not enough to constrain this parameter. An analysis with the same error scale for all parameters (Figure S4 in the Supplementary material), showed that K_N, $\dot{k}_{E_N}$, $j_{E_N M}$, and $j_{E_C M}$ are the most sensitive parameters to the different types of data used for estimation. Overall the results highlight the complementary role and need for nutrient uptake and starvation data to better constrain model parameters (Fig. 7).

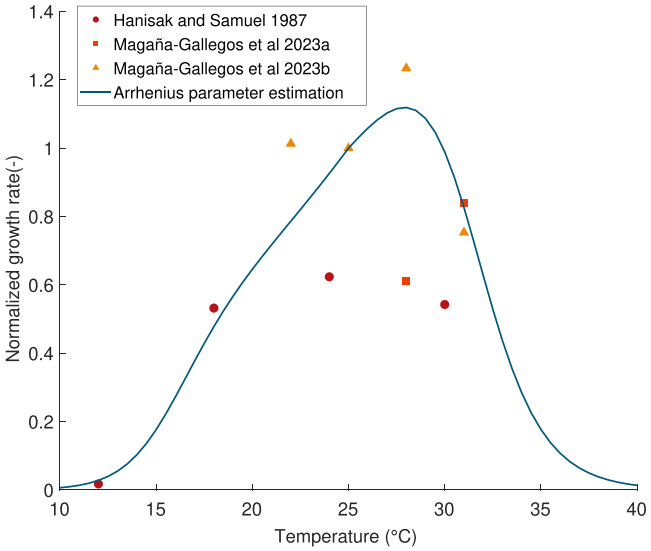

Fig. 4. Holopelagic *Sargassum* spp. normalized growth rate (solid blue line) estimated from three datasets under different culture temperatures (colored symbols).

4. Discussion

In this paper we developed a multi-reserve DEB model to describe the growth dynamics of the holopelagic *Sargassum* spp. morphotype, *S. fluitans* var. *fluitans*. The model explicitly accounts for the absorption of light, carbon and nitrogen by using one reserve for each nutrient. Each reserve is then processed to pay for maintenance costs and to grow. The model structure was based on previous macroalgal models (Lavaud et al., 2020; Venolia et al., 2020), and we also conducted a literature review to select available experimental datasets specific to holopelagic *Sargassum* spp. physiology and used these to estimate some of the model parameters.

4.1. Evaluation of available datasets and sources of uncertainty

Experimental datasets on the physiology of the three holopelagic *Sargassum* morphotypes are limited and often highly variable. Differences between studies, such as the season of collection of organisms,

Table 4
Model core and auxiliary parameters for *S. fluitans* at T_{ref} = 20 °C (= 293.15 K). MRE = 0.026, SMAE = 0.024, and SMSE = 0.002 [a].

Symbol	Unit	Description	Value	Source
Core parameters				
$j_{E_N Am}$	mol M_{E_N} mol M_V^{-1} h^{-1}	Maximum volume specific nitrogen assimilation	8.4169e^{-5}	Estimated
K_N	mol N L^{-1}	Half-saturation concentration for nitrogen NO_3^- and NH_4^+ uptake	1.043e^{-7}	Estimated
j_{Cm}	mol CO_2 mol M_V^{-1} h^{-1}	Maximum volume specific CO_2 uptake rate	0.0074	Venolia et al. (2020)
K_C	mol CO_2 L^{-1}	Half-saturation concentration for CO_2 uptake	4e^{-7}	Venolia et al. (2020)
ρ_{PSU}	mol PSU mol M_V^{-1}	Photosynthetic unit (PSU) density	0.5	Venolia et al. (2020)
ϵ_I	m^2 mol PSU^{-1}	Effective photon binding efficiency, compound parameter $\epsilon_I = \alpha_I \dot{b}_I$ (See Appendix A)	0.3487	Estimated
$\dot{k}_I$	mol γ mol PSU^{-1} h^{-1}	Dissociation rate of photosynthetic products	0.0718	Estimated
y_{IE_C}	mol γ mol $M_{E_C}^{-1}$	Yield of C reserve per photon	10	Venolia et al. (2020)
y_{CE_C}	mol CO_2 mol $M_{E_C}^{-1}$	Yield of C reserve per CO_2	1	Venolia et al. (2020)
y_{OI}	mol O_2 mol γ^{-1}	Yield factor of O_2 to photon	0.125	Venolia et al. (2020)
$j_{E_C Am}$	mol M_{E_C} mol M_V^{-1} h^{-1}	Maximum volume specific carbon assimilation	0.2774	Venolia et al. (2020)
$\dot{k}_{E_N}$	h^{-1}	N reserve turnover rate	0.2147	Estimated
$\dot{k}_{E_C}$	h^{-1}	C reserve turnover rate	0.0184	Estimated
$j_{E_N M}$	mol M_{E_N} mol M_V^{-1} h^{-1}	Volume specific maintenance cost paid by N reserve	2.6532e^{-6}	Estimated
$j_{E_C M}$	mol M_{E_C} mol M_V^{-1} h^{-1}	Volume specific maintenance cost paid by C reserve	9.6917e^{-7}	Estimated
$y_{E_N V}$	mol M_{E_N} mol M_V^{-1}	Yield factor of N reserve to structure	0.04	Venolia et al. (2020)
$y_{E_C V}$	mol M_{E_C} mol M_V^{-1}	Yield factor of C reserve to structure	1.25	Lavaud et al. (2020)
κ_{Ei}	–	Fraction of rejection flux incorporated back in i-reserve	0.9	Venolia et al. (2020)
T_A	K	Arrhenius temperature	6603	Estimated
T_H	°C (K)	Upper boundary of temperature tolerance	31.15 (304.3)	Estimated
T_L	°C (K)	Lower boundary of temperature tolerance	15.75 (288.9)	Estimated
T_{AH}	K	Arrhenius temperature for the rate of decrease at T_H	58 010	Estimated
T_{AL}	K	Arrhenius temperature for the rate of decrease at T_L	54 620	Estimated
w_V	g mol^{-1}	Molar weight of structure	29.93	Venolia et al. (2020)
w_{E_N}	g mol^{-1}	Molar weight of N reserve	40	Sum of elements
w_{E_C}	g mol^{-1}	Molar weight of C reserve	30	Sum of elements
w_O	g mol^{-1}	Molar weight of O_2	32	–
Auxiliary parameters [b]				
ψ_S	g_w cm^{-2}	Mass-to-surface ratio	0.04737	Estimated
ϕ_{dw}	g_d g_w^{-1}	Dry-to-wet weight ratio	0.178	pers. comm.
x_{ash}	% g_d	Mean ash proportion	0.4	Machado et al. (2022), Tonon et al. (2022)
x_{moist}	% g_d	Mean moisture proportion	0.1	Machado et al. (2022), Tonon et al. (2022)

[a] MRE= Mean Relative Error, SMAE= Symmetric Mean Absolute Error , SMSE= Symmetric Mean Squared Error.
[b] The units g_d and g_w stands for grams dry and wet weight respectively.

experimental setup, environmental treatments, and the duration of the experiments, make it challenging to compare results between studies (Hatt et al., 2025). Replicating experiments using the model may also be complicated when key environmental variables are not available. For example, both *in-situ* and some *ex-situ* cultures are subject to environmental conditions at sea (e.g. the nutrient concentrations in systems supplied with unfiltered flowing water), making it hard to quantify nutrient inputs and their effects on algal growth and survival (Corbin and Oxenford, 2023). Additionally, initial and final tissue nutrient content is not known (Magaña-Gallegos et al., 2023b), it is hard to establish if differences in observed growth rates, for example, are fully due to the different experimental treatments (temperatures) or partly to differences in the initial conditions of the organisms (Magaña-Gallegos et al., 2023a). Moreover, some experimental results could not be directly integrated because of differences in experimental units and the DEB framework. For instance, organism size may be expressed as surface area (cm^2) or length (cm) (Vásquez-Elizondo et al., 2023; Schell et al., 2024), whereas our multi-reserve model relies on dry weights, as it is used to describe an organism's chemical composition and mass balance (Kooijman, 2010).

We also wish to highlight that another source of uncertainty arises from the information about the elemental and compound composition of the organisms. Indeed, the percentage of ash reported for holopelagic *Sargassum* spp. samples (Machado et al., 2022; Tonon et al., 2022; Lapointe et al., 2021) is higher than other *Sargassum* spp. from which epibionts were removed (Kumar et al., 2015; Winarni et al., 2021). Although holopelagic *Sargassum* spp. samples were cleaned (Machado et al., 2022; Tonon et al., 2022), these may account for macro debris (e.g. plastics) or other associated fauna, not necessarily the removal of epibionts (Hatt et al., 2024). Despite the variability between datasets and the need for simplifying assumptions, the model was able to reproduce the main patterns observed for *S. fluitans* var. *fluitans*. In particular it capture the response to temperature and the photosynthetic production.

4.2. Model structure and parameter estimation

While our *Sargassum* DEB model generally captures the trends in experimental observations, slight deviations remain. These discrepancies may arise from parameter identifiability issues, but they could also result from the model structure not fully capturing all relevant biological processes. For instance, photo-acclimation and photoinhibition, described as important processes for holopelagic *Sargassum* spp. acclimated to low light conditions (Vásquez-Elizondo et al., 2023), are not included in the current model structure. This could limit the model's capacity to reproduce the light-dependent dynamics. Photo-acclimation could be included by modifying parameters dynamically as proposed by Papadakis et al. (2005), or by introducing additional parameters to account for the photoinhibition process (Lorena et al., 2010). Although these additions would increase the model complexity, they may help reduce deviations between observations and model predictions.

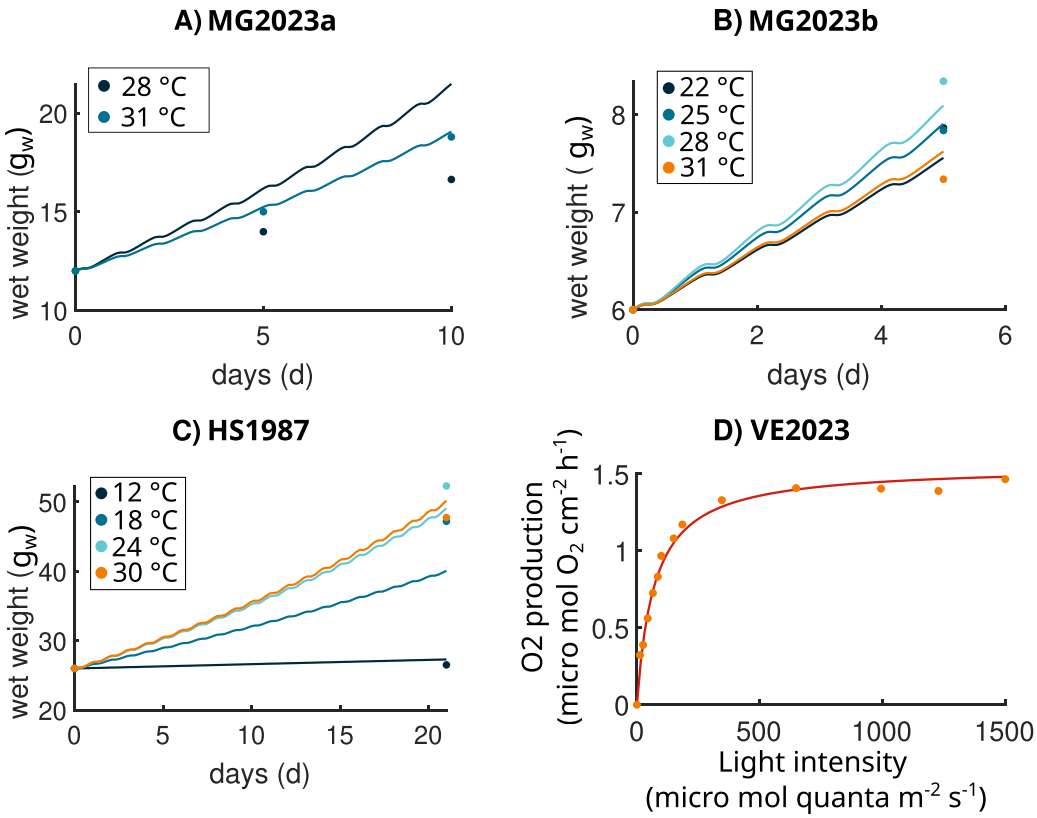

Fig. 5. Experimental data on *Sargassum fluitans* var. *fluitans* (shown as dots) used for parameter estimation, together with model predictions (shown as continuous lines) for each dataset. Wet weight evolution with time from (A) Magaña-Gallegos et al. (2023b) (B) Magaña-Gallegos et al. (2023a) (C) Hanisak and Samuel (1987) (not used for parameter estimation). (D) Oxygen production rate vs. light intensity (prediction in red, data in orange) from algae acclimated to high light conditions from Figure 1a, Vásquez-Elizondo et al. (2023).

When comparing our results with the initial parameters values, the resulting estimated parameters show a lower assimilation when compared to the benthic brown algae *Saccharina latissima*, slightly higher N and C reserve turnover rates, and similar values of somatic maintenance. The values of the estimated parameters are in the same range as the other brown macroalgae species, and they capture the ranges of growth rates and wet weight evolution observed in holopelagic *Sargassum* spp. experiments, as well as the C:N ratios (Lapointe, 1995; Magaña-Gallegos et al., 2023a,b).

The estimation of DEB model parameters is not easy, particularly in the case of a multi-reserve model, where the number of parameters increases compared to a single reserve animal model (Kooijman, 2010). This is particularly true when data is scarce or does not cover all critical physiological processes. When conducting the DEB parameters calibration, if the data does not contain the necessary information to constrain parameters, then the parameter values can be unrealistic, resulting in erroneous predictions (Lika and Kooijman, 2024). This may indicate a problem of parameter non-identifiability (Wieland et al., 2021), raising the issue treated here: data available may not be informative enough to determine accurate parameters. To address this issue, we proposed a protocol based on the virtual ecologist approach to determine parameters identifiability. The quantitative approach was inspired by a protocol proposed to analyze the effect of data gaps on parameter estimation (Accolla et al., 2020). However, other more computational intensive methods, such as confidence intervals or profile likelihood analysis, could complement our approach (Raue et al., 2010; Marques et al., 2019; Lika and Kooijman, 2024).

4.3. Experimental data needed to improve parameter estimation

We found that measurements of nutrient uptake and assimilation into the N reserve could be critical for a more accurate estimation of our model parameters. In previous DEB models applied to macroalgae, nutrient uptake was included in the datasets used for estimation (Lavaud et al., 2020; Venolia et al., 2020). Conducting this type of experiment for each holopelagic *Sargassum* spp. morphotypes would be a major achievement.

When excluding photosynthesis data from the parameter estimation, we found that photosynthesis-related parameters showed a much higher estimation error. In our case, only one dataset provided information about the photosynthetic response (Vásquez-Elizondo et al., 2023). In this study, algae were acclimated for a long period to the lab conditions, therefore possibly not fully reflecting the *in-situ* response of *Sargassum* spp. to different light intensities (Davison, 1991; Falkowski and LaRoche, 1991). Besides, previous DEB studies dedicated to macroalgae incorporated several datasets of the photosynthetic response at different temperatures and different light intensities (Lavaud et al., 2020; Venolia et al., 2020). Having this information for holopelagic *Sargassum* spp. would therefore help better calibrate the model.

The reserve turnover parameters were better estimated when including data on nitrogen uptake and starvation. The starvation experiments included *"virtual" observed data* on wet weight and C:N:P ratios over time. During starvation, the ratio of reserve to structure varies, causing an increase in the overall C:N ratios of the organism within the first 10 days, after which the ratios stabilize. This type of data is particularly informative for parameters controlling reserve dynamics, as the reserves turnover rate (Kooijman, 2010). In the case of the parameters of somatic maintenance cost, for algae this includes the turnover of structure, maintenance of cellular gradients, and the maturity maintenance (Kooijman, 2010). Lavaud et al. (2020) showed that starvation experiments helped to calibrate the maintenance cost for nitrogen and carbon in their DEB model of a green macroalga. In our case, starvation data improved the estimation of the nitrogen

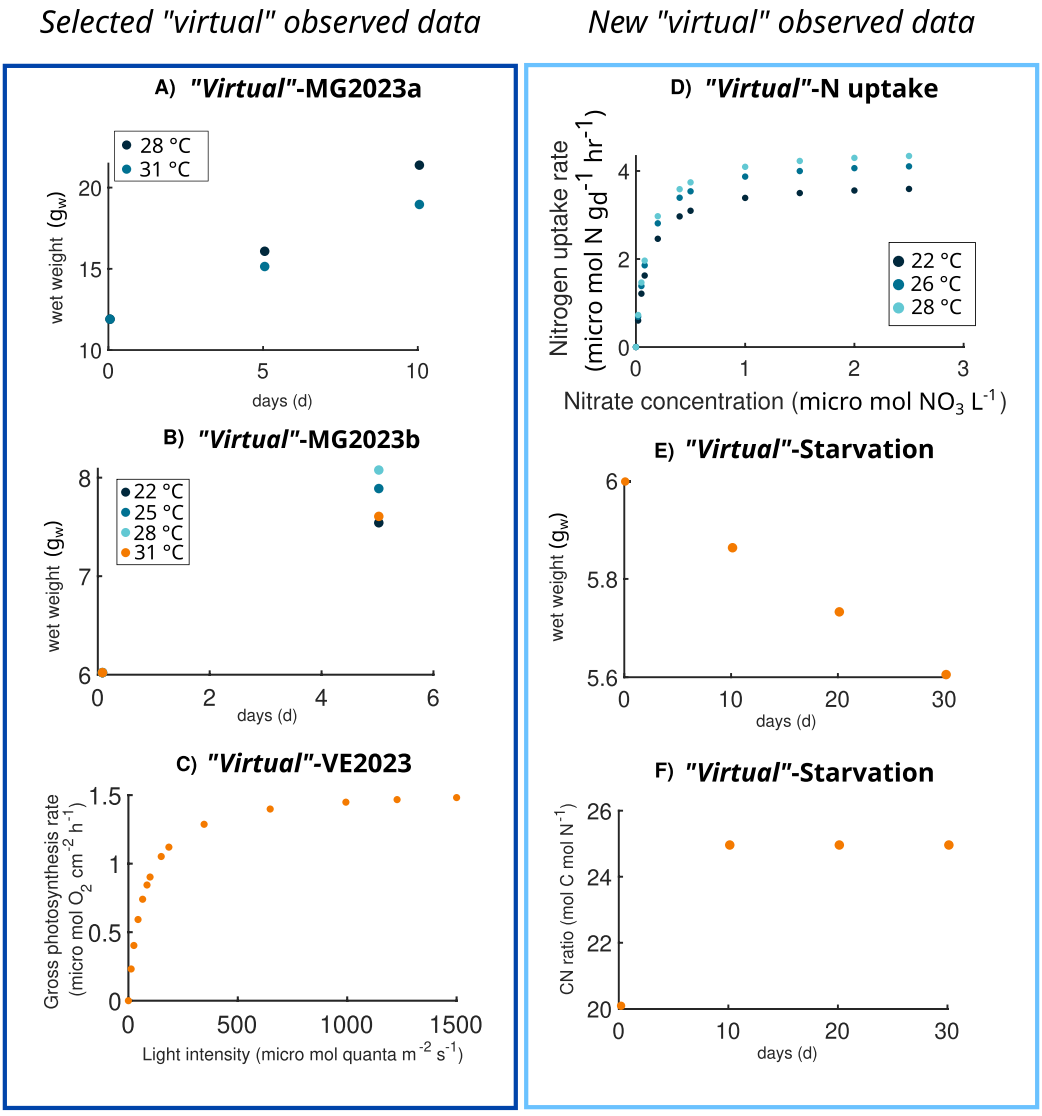

Fig. 6. Left: *Selected "virtual" observed data* created using the forcing conditions and initial conditions to mimic the available data. (A) Magaña-Gallegos et al. (2023a), (B) Magaña-Gallegos et al. (2023b), and (C) Vásquez-Elizondo et al. (2023). Right: *New "virtual" observed data* (D) N uptake data at 24, 26, and 28 °C; E and F) Wet weight and C:N ratio over time at 25 °C for the starvation experiment (forcing conditions set with irradiance at 200 μmol quanta m^{-2} s^{-1}, and N and CO_2 at $1e^{-10}$ mol L^{-1}).

somatic maintenance, but not of carbon somatic maintenance alone, possibly due to a lower variability of the carbon reserve in starvation conditions compared to the nitrogen reserve (See Supplementary material). Additionally, the "virtual" observed data was created simulating low light conditions with a photoperiod effect, however further studies with no light could improve the identifiability of this parameters. Overall, measuring the variability of C:N:P ratios over time and the weight evolution in starvation conditions would also be an important improvement to understand holopelagic *Sargassum* spp. physiology.

Data uncertainties present significant challenges for bioenergetic modeling of holopelagic *Sargassum* spp. While we worked with the available datasets and made explicit assumptions about missing information, our analysis highlights key gaps (information about the initial conditions, forcing variables and different physiological processes), which would improve our understanding on holopelagic *Sargassum* spp. physiology. Future experimental studies would therefore enable more robust parameters estimation and improve model predictive capacity. Until such comprehensive datasets become available, model predictions should be interpreted with caution.

The virtual ecologist approach used in this study to assess parameter identifiability provides a useful framework to guide data acquisition planning by linking modeling and experimental work (Kooijman et al., 2024; Jakeman et al., 2024). It encourages an integrated modeling process with collaboration between modelers and empiricists, helping modelers better understand the feasible experiments and sampling given time and cost constraints, while empiricist gain a clearer view of the predictive capacity of the models and the type of information that can be extracted from data by models (Section 4, point 9 Jakeman et al., 2024; Zurell et al., 2010). This is particularly useful for designing experiments aimed at better understanding the physiology of organisms and reducing parameter uncertainty (Section 4, point 14 Jakeman et al., 2024), in our case for holopelagic *Sargasssum* spp., within a DEB modeling framework. More broadly, modeling studies could benefit from such virtual ecologist approaches to improve experimental data and model interpretation and facilitate the transfer of knowledge to studies on higher levels of organization (Bourdaud et al., 2024).

4.4. Directions for model improvements

Growth limitation of holopelagic *Sargassum* spp. when phosphorus is scarce it is well documented (Lapointe et al., 2021; Lapointe, 1986),

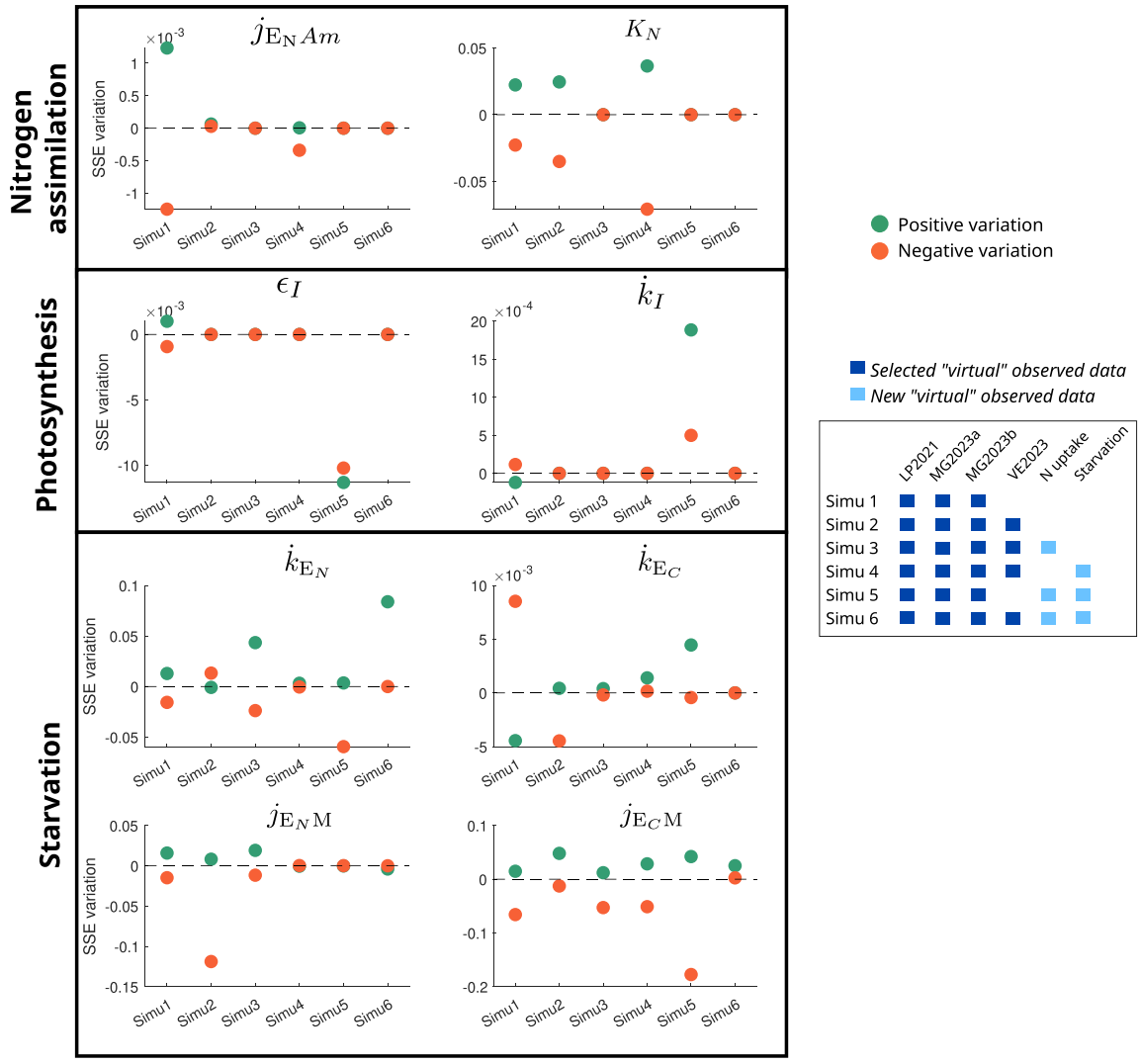

Fig. 7. Error (SSE) values obtained for every estimated parameter depending on combinations of *"virtual" observed data* used for estimation (Simu *i*, box). The orange dots in the graphs represent the resulting error for the estimated parameters initialized with *"true"* parameters at −10% and the green dots at +10%. The labels used for the *"virtual" observed data* are LP2021 for Lapointe et al. (2021), MG2023a for Magaña-Gallegos et al. (2023a), MG2023b for Magaña-Gallegos et al. (2023b), and VE2023 for Vásquez-Elizondo et al. (2023). See Table 3 for more information on each dataset.

and similar effects have been reported for iron (Leemans et al., 2025). In the case of phosphorus limitation, sargassum can assimilate arsenic through the same uptake pathway (Gobert et al., 2022). In our model, a third reserve, specific to phosphorus could be added (Grossowicz et al., 2017), as well as one for micronutrients such as iron. Such extension would allow simulating the observed growth limitation by P and Fe, and the substitution of P by arsenic, through a substitutable SU in which arsenic is assimilated but not mobilized (Kooijman, 2010). However, including more reserves demands additional parameters and the need for more data on the corresponding processes in order to constrain parameter estimation. Further extension could also include different temperature effects on physiological processes. This is of particular interest, as different temperature responses have been observed for growth and photosynthesis in holopelagic *Sargassum* (Hatt et al., 2025).

In this study we estimated parameters using datasets from the tropical Atlantic population of *S. fluitans* var. *fluitans* morphotype only. The next step will be to include the two other holopelagic *Sargassum* morphotypes to better understand the physiological differences across morphotypes and how these contribute to the different growth rates reported (Changeux et al., 2023; Corbin and Oxenford, 2023; Payne et al., 2024). Also, to study the spatiotemporal variability of holopelagic *Sargassum* spp. at larger spatial scales, one should consider the potential differential physiological responses according to the different geographical zones, and thereby environmental conditions (Hatt et al., 2025). It has been shown that holopelagic *Sargassum* spp. reproduces by fragmentation/cloning. As a result, there are no differential evolutionary processes that can explain different physiological responses across populations in the tropical Atlantic and Sargasso sea. However, regional acclimation or even inter-individual differences (due to local environmental heterogeneity or stochastic processes) could be interesting points to further study. In this study and generally, DEB theory represents an average organism, however DEB theory can also be applied with specific parameters for each individual or it can be used to study the differences between the two populations (Monaco et al., 2019; Oliveira et al., 2024).

Finally, this DEB multi-reserve model could also be coupled with particle-tracking approaches to explore the spatial and interannual variability in dispersal and accumulation of Sargassum between regions and years. Sun et al. (2026) studied *Sargassum horneri* blooms using Droop's quota model, to simulate growth as a function of nutrient concentrations, coupled with a particle tracking model. Similarly, Jouanno et al.

(2025) and Podlejski et al. (2024) have used these approaches, providing valuable insights into the spatiotemporal dynamics of holopelagic *Sargassum*. However, Droop's quota model is a special case of a multi-reserve DEB model with no maintenance costs (Kooijman, 2010). The multi-reserve DEB model developed here, which includes maintenance cost, is particularly relevant for studying organism physiology and survival under limiting conditions. Ultimately, this type of model coupled with a practical tracking model will allow a better understanding of the spatiotemporal dynamics of holopelagic *Sargassum* spp., as well as other bloom forming algae.

5. Conclusions

This study demonstrates that the growth dynamics and physiological processes of holopelagic *Sargassum* spp. can be described using a multi-reserve DEB model. However, building and calibrating a new species-specific model with insightful parameters is highly dependent on the availability of informative data. Our analysis shows data gaps and differences between holopelagic *Sargassum* spp. experimental results for the same physiological response variable (e.g. temperature). Additionally, including data on nutrient uptake, starvation, and photosynthesis, improves parameters identifiability significantly. We also demonstrated how using the virtual ecologist approach we can quantitatively assess how different types of experiments contain more information for improving parameter estimation. Our work shows that even with limited data, the DEB model provides insights into the dynamics of *Sargassum* spp., but targeted experiences covering a broad range of environmental conditions are essential to improve the model's calibration and predictive capacity. Future efforts should focus on designing targeted experiments collectively between modelers and experimental researchers to gain insights into *Sargassum* spp. physiological responses.

CRediT authorship contribution statement

María-José Lagunes: Writing – review & editing, Writing – original draft, Visualization, Methodology, Investigation, Formal analysis, Conceptualization. **Gonçalo M. Marques:** Writing – review & editing, Validation, Methodology. **Evelyn R. Salas-Acosta:** Writing – review & editing, Validation, Resources, Conceptualization. **Roman M. Vásquez-Elizondo:** Writing – review & editing, Validation, Resources. **Thierry Thibaut:** Writing – review & editing, Resources. **Daniel Robledo:** Writing – review & editing, Resources. **Solène Connan:** Writing – review & editing, Resources. **Valérie Stiger-Pouvreau:** Writing – review & editing, Resources. **Léo Berline:** Writing – review & editing, Supervision, Project administration, Funding acquisition. **Christophe Lett:** Writing – review & editing, Supervision, Conceptualization. **Laure Pecquerie:** Writing – review & editing, Validation, Supervision, Methodology, Conceptualization.

Declaration of competing interest

The authors declare that they have no known competing financial interests or personal relationships that could have appeared to influence the work reported in this paper.

Acknowledgments

This work is part of the BIOMAS project (https://biomas.osupytheas.fr/) funded by the ANR program SARGASSUM - 2022 (ANR-22-SARG-0003).

Table 5
Compounds notation and units used thought model equations and parameters.

Compounds	Notation	Unit variable
Light	I	mol γ
Oxygen	O	mol O_2
N pool	N	mol N
Carbon	C	mol CO_2
N reserve	E_N	mol M_{E_N}
C reserve	E_C	mol M_{E_C}
Structure	V	mol M_V

Appendix A. Model equations

Metabolic processes represented as DEB model equations which describe transformations of different compounds described in Table 5.

Nutrient assimilation Nitrogen uptake is described in the model as a Michaelis–Menten reaction, with the equation:

$$j_{E_N A} = j_{E_N Am} \frac{[N]}{K_N + [N]} \tag{2}$$

in mol M_{E_N} mol M_V^{-1} h^{-1} With $j_{E_N Am}$ the maximum volume specific nitrogen assimilation and K_N, the half-saturation for N, and [N] the nitrogen concentration (in this work, we do not distinguish the different nitrogen compounds).

The assimilation of carbon involves two processes: light uptake and inorganic carbon uptake. The mechanism of carbon uptake is based on the concept of complementary parallel SUs see Kooijman (2010, section 3.7.3) and Poggiale et al. (2010) for more details. Following Lavaud et al. (2020), the first SU describes the specific relaxation rate j_I. Photos are captured and transformed into NADPH with simple SU dynamics (as described in Lorena et al. (2010) but without photoinhibition). The second SU describes the inorganic carbon uptake as a Michaelis–Menten function j_C, and the thirds SU dynamics corresponds to a complementary parallel SU in which the products of the SU1 and SU2 are taken and transformed in glucose. The dynamics of carbon uptake are as follows (Eqs. (3) and (4) and see the equation in Box I):

$$j_I = \frac{\rho_{PSU}\, \epsilon_I\, I}{1 + \frac{\epsilon_I\, I}{\dot{k}_I}} \text{ in mol } \gamma \text{ mol } M_V^{-1} \text{ h}^{-1} \tag{3}$$

$$j_C = j_{C_m} \frac{[C]}{K_C + [C]} \text{ in mol } CO_2 \text{ mol } M_V^{-1} \text{ h}^{-1} \tag{4}$$

where ρ_{PSU}, corresponds to photosynthetic unit density ϵ_I, the compound parameter $\epsilon_I = \alpha_I \dot{b}_I$, the effective photon binding efficiency with $\dot{b}_I$ binding probability of a photon to a free light PSU per section and α_I the specific photon arrival cross section, and $\dot{k}_I$, the dissociation rate of photosynthetic products. j_{Cm} represents the volume maximum specific CO_2 uptake rate and K_C, the half-saturation constant of C. $j_{E_C A}$, describes the flux of C entering the m_{E_C} reserve density. The yield of C obtained by the yield of C per compound of NADPH and CO2, is obtained with y_{IE_C} and y_{CE_C}. For a more detailed description of the photosynthesis, see the Supplementary material.

Reserve dynamics Energy and mass of each reserve will then be mobilized to pay for somatic and maturity maintenance costs and growth, with maintenance having priority over growth and being proportional to structural volume. For each reserve we obtain the specific mobilized flux $j_{E_i C}$ (with i = N or C) as

$$j_{E_i C} = m_{E_i} \left(\dot{k}_{E_i} - \dot{r} \right) \text{ in mol } M_{E_i} \text{ mol } M_V^{-1} \text{ h}^{-1} \tag{6}$$

with $\dot{r} = \frac{1}{M_V} \frac{dM_V}{dt}$ the specific growth rate in h^{-1} and $\dot{k}_{E_i}$, the i-reserve turnover rate. And the maintenance rate to pay for maintenance costs is obtained as,

$$j_{E_i}^{M_i} = \min\left(j_{E_i C}, j_{E_i M}\right) \text{ in mol } M_{E_i} \text{ mol } M_V^{-1} \text{ h}^{-1} \tag{7}$$

$$j_{E_C A} = \left(\frac{1}{j_{E_C Am}} + \frac{1}{j_C / y_{CE_C}} + \frac{1}{j_I / y_{IE_C}} - \frac{1}{j_I / y_{IE_C} + j_C / y_{CE_C}} \right)^{-1} \text{ in mol } M_{E_C} \text{ mol } M_V^{-1} \text{ h}^{-1} \quad (5)$$

Box I.

where $j_{E_i M}$, corresponds to the volume specific maintenance cost that must be paid by each reserve.

To obtain the mobilization rate the net specific growth rate $\dot{r}$ is calculated via an implicit function. To obtain this value at each time the Newthon-Raphson method is used to find the root of the function according to the flux values. To do so, we use the DEB-tool package as in Lavaud et al. (2020).

Growth dynamics

The fraction of mobilized reserve which is not used to pay for maintenance will be then send to the growth SU, where all flux are merged as a parallel complementary SU.

$$j_{E_i G} = j_{E_i C} - j_{E_i}^{M_i} \text{ in mol } M_{E_i} \text{ mol } M_V^{-1} \text{ h}^{-1} \quad (8)$$

The specific growth flux will then be:

$$j'_{VG} = \left(\sum_i \left(\frac{j_{E_i G}}{y_{E_i V}} \right)^{-1} - \left(\sum_i \frac{j_{E_i G}}{y_{E_i V}} \right)^{-1} \right)^{-1} \text{ in h}^{-1} \quad (9)$$

Therefore when considering C and N reserves,

$$j'_{VG} = \left(\left(\frac{j_{E_C G}}{y_{E_C V}} \right)^{-1} + \left(\frac{j_{E_N G}}{y_{E_N V}} \right)^{-1} - \left(\frac{j_{E_C G}}{y_{E_C V}} + \frac{j_{E_N G}}{y_{E_N V}} \right)^{-1} \right)^{-1} \text{ in h}^{-1} \quad (10)$$

with $y_{E_i V}$, the yield factor of i-reserve to create 1 C-mol of structure.

When considering different assimilation pathways and as stated from the parallel complementary SU, when there is one liming nutrient the non-limiting nutrient will occupy is specific binding site until the limiting nutrient binding sites are occupied. The excess non-limiting nutrient will be rejected from the growth SU. From this rejected flux, there is κ_{Ei} fraction for this flux to be sent back to their specific reserve or 1 - κ_{Ei} to be excreted into the environment. The rejection flux is expressed as:

$$j_{E_i r} = j_{E_i G} - y_{E_i V} j_{VG} \text{ in mol } M_{E_i} \text{ mol } M_V^{-1} \text{ h}^{-1} \quad (11)$$

Additionally, if one nutrient is not sufficient to pay for the specific maintenance cost associated to its reserve, structure can be broken down to pay for the remaining cost, meaning that growth rate $\dot{r}$, can be negative.

$$j'_{VM_i} = (j_{E_i M} - j_{E_i}^{M_i}) y_{E_i V}^{-1} \quad (12)$$

The sum of this flux is expressed as $j_V^{'M} = \sum_i j'_{VM_i}$ in h^{-1}

Model dynamics

$$\frac{dm_{E_C}}{dt} = j_{E_C A} - j_{E_C C} + (\kappa_{E_C} j_{E_C r}) - (\dot{r} m_{E_C}) \text{ in mol } M_{E_C} \text{ mol } M_V^{-1} \text{ h}^{-1} \quad (13)$$

$$\frac{dm_{E_N}}{dt} = j_{E_N A} - j_{E_N C} + (\kappa_{E_N} j_{E_N r}) - (\dot{r} m_{E_N}) \text{ in mol } M_{E_N} \text{ mol } M_V^{-1} \text{ h}^{-1} \quad (14)$$

$$\frac{dM_V}{dt} = \dot{r} M_V \quad \text{in mol } M_V \text{ h}^{-1} \quad (15)$$

As mentioned in Section 2 (Table 1), the model state variables include M_{E_N}, M_{E_C}, and M_V. The first two correspond to the nitrogen and carbon reserves, respectively, and are related to Eqs. (13) and (14). These variables represent total reserve mass, while the reserve densities used in the equation are given by $m_{E_i} = M_{E_i} / M_V$ (Kooijman, 2010).

Appendix B. Arrhenius equation

As stated before, temperature has an effect over an organism's physiology and uptake rates. Indeed, all organisms' metabolic rates are dependent on enzymes which are affected by temperature. This can be modeled using the Arrhenius relationship described in Kooijman (2010). Moreover, the enzyme's reaction rate is regulated at high and low temperatures (described as the species thermal tolerances) where enzymes are partially deactivated (Schoolfield et al., 1981). To account for this behavior, the extend Arrhenius equation is implemented to correct temperature dependent rates, as following:

$$\dot{k}(T) = \dot{k}_{\text{ref}}\, c(T) \quad (16)$$

where $\dot{k}_{ref}$ represents metabolic rates at the reference temperature T_{ref} defined for the species and $c(T)$, is the correction factor of temperature defined as:

$$c(T) = \exp\left(\frac{T_A}{T_{ref}} - \frac{T_A}{T} \right) \left(1 + \exp\{ \frac{T_{AL}}{T_{ref}} - \frac{T_{AL}}{T_L} \} + \exp\{ \frac{T_{AH}}{T_H} - \frac{T_{AH}}{T_{ref}} \} \right) \left(1 + \exp\{ \frac{T_{AL}}{T} - \frac{T_{AL}}{T_L} \} + \exp\{ \frac{T_{AH}}{T_H} - \frac{T_{AH}}{T} \} \right)^{-1} \quad (17)$$

At each time step and for each temperature (T), this equation is calculated using the temperature related parameters (T_A, T_H, T_L, T_{AH}, and T_{AL}, see Table 4), which are then used to modify the following model parameters: j_{C_m}, $\dot{k}_I$, $j_{E_C Am}$, $j_{E_N Am}$, $\dot{k}_{E_C}$, $\dot{k}_{E_N}$, $j_{E_C M}$ and $j_{E_N M}$ (also defined in Table 4).

Appendix C. Linking model state variables to observable variables

DEB theory generality and applicability to different organisms comes with a cost: the model's state variables are not directly measurable. However, to link these variables with commonly measured quantities as wet weight, O_2 production or C:N:P ratios, auxiliary parameters are used (Table 4) (Lika et al., 2011; Nisbet et al., 2012).

The total biomass of an organism is the resulting addition of each reserve and the structure. This can be transformed in dry weight as:

$$W_{d_\odot} = M_V (w_V + (m_{E_C} w_{E_N}) + (m_{E_C} w_{E_C})) \quad (18)$$

in grams of organic dry weight. Organic dry weight can then be transformed to wet weight. To do this, we should consider that the total dry weight represents the sum of the organic and inorganic compounds. Therefore, to obtain the total dry weight we first add the inorganic proportion as:

$$W_d = W_{d_\odot} / (1 - x_{moist} - x_{ash}) \quad (19)$$

with x_{moist} and x_{ash}, the percentage of inorganic matter g_d. Finally, the total dry weight can be transformed into wet weight, according to the dry weight/wet weight ratio (ϕ_{dw}).

Growth rate was calculated as described by Hanisak and Samuel (1987), with dry weight transformed into wet weight:

$$\dot{r}_D = \frac{\log_2(W_{w_f} / W_{w_0})}{t} \quad (20)$$

in doublings per day. With t, time in days. With W_{w_f} and W_{w_0}, the final and initial wet weight, respectively. This is equivalent to RGR or SGR reported in the literature.

Additionally, the C:N:P ratios were calculated following:

$$\begin{aligned} C_{\text{total}} &= n_{CV} M_V + n_{CE_C} M_{E_C} \\ N_{\text{total}} &= n_{NV} M_V + n_{NE_N} M_{E_N} \\ P_{\text{total}} &= x_{PV} M_V \end{aligned} \tag{21}$$

$$\begin{aligned} \text{CN}_{\text{total}} &= \frac{C_{\text{total}}}{N_{\text{total}}} \quad \text{mol C mol N}^{-1} \\ \text{CP}_{\text{total}} &= \frac{C_{\text{total}}}{P_{\text{total}}} \quad \text{mol C mol P}^{-1} \\ \text{NP}_{\text{total}} &= \frac{N_{\text{total}}}{P_{\text{total}}} \quad \text{mol N mol P}^{-1} \end{aligned} \tag{22}$$

Finally, the oxygen production rate was estimated as:

$$j_O = j_I \left(\frac{M_V}{W_{d_\mathcal{O}}}\right) y_{OI}\ \psi_s\ \phi_{dw} \tag{23}$$

in mol O_2 cm^{-2} h^{-1}

Appendix D. Supplementary data

Supplementary material associated with this article can be found in the attached files. The associated codes used for analysis and to generate figures can be found in the Github repository associated to this paper (Lagunes and Pecquerie, 2025).

Supplementary material related to this article can be found online at https://doi.org/10.1016/j.ecolmodel.2026.111578.

Data availability

We have shared the link to the code in the Supplementary material section and as a separate file.

SargaDEB_SFF_NeededExperiments (Original data) (Github)

References

Accolla, C., Vaugeois, M., Rueda-Cediel, P., Moore, A., Marques, G.M., Marella, P., Forbes, V.E., 2020. DEB-tox and Data Gaps: Consequences for individual-level outputs. Ecol. Model. 431, 109107. http://dx.doi.org/10.1016/j.ecolmodel.2020.109107, URL: https://linkinghub.elsevier.com/retrieve/pii/S0304380020301794.

Berline, L., Ody, A., Jouanno, J., Chevalier, C., André, J.-M., Thibaut, T., Ménard, F., 2020. Hindcasting the 2017 dispersal of *Sargassum* algae in the Tropical North Atlantic. Marine Poll. Bull. 158, 111431. http://dx.doi.org/10.1016/j.marpolbul.2020.111431, URL: https://linkinghub.elsevier.com/retrieve/pii/S0025326X2030549X.

Bourdaud, P., Niquil, N., Araignous, E., Cabral, H., Carpentier, A., Drouineau, H., Lobry, J., Pecquerie, L., Saint-Béat, B., Lassalle, G., Vagner, M., 2024. Linking individual experiments and multiscale models to simulate physiological perturbations on aquatic food webs. Front. Ecol. Evol. 12, 1400936. http://dx.doi.org/10.3389/fevo.2024.1400936, URL: https://www.frontiersin.org/articles/10.3389/fevo.2024.1400936/full.

Brooks, M., Coles, V., Hood, R., Gower, J., 2018. Factors controlling the seasonal distribution of pelagic *Sargassum*. Mar. Ecol. Prog. Ser. 599, 1–18. http://dx.doi.org/10.3354/meps12646, URL: https://www.int-res.com/abstracts/meps/v599/p1-18/.

Chambon, B., 2022. Quantification de la relation taille - biomasse de trois morphotypes de sargasses pélagiques par traitement d'image. Technical Report, Aix-Marseille University.

Changeux, T., Berline, L., Podlejski, W., Guillot, T., Stiger-Pouvreau, V., Connan, S., Thibaut, T., 2023. Variability in growth and tissue composition (CNP, natural isotopes) of the three morphotypes of holopelagic *Sargassum*. Aquat. Bot. 187, 103644. http://dx.doi.org/10.1016/j.aquabot.2023.103644, URL: https://linkinghub.elsevier.com/retrieve/pii/S0304377023000293.

Corbin, M., Oxenford, H.A., 2023. Assessing growth of pelagic sargassum in the Tropical Atlantic. Aquat. Bot. 187, 103654. http://dx.doi.org/10.1016/j.aquabot.2023.103654, URL: https://linkinghub.elsevier.com/retrieve/pii/S0304377023000396.

Davison, I.R., 1991. Environmental effects on algal photosynthesis: temperature. J. Phycol. 27 (1), 2–8. http://dx.doi.org/10.1111/j.0022-3646.1991.00002.x, URL: https://onlinelibrary.wiley.com/doi/10.1111/j.0022-3646.1991.00002.x.

Falkowski, P.G., LaRoche, J., 1991. Acclimation to spectral irradiance in algae. J. Phycol. 27 (1), 8–14. http://dx.doi.org/10.1111/j.0022-3646.1991.00008.x, URL: https://onlinelibrary.wiley.com/doi/10.1111/j.0022-3646.1991.00008.x.

Fidai, Y.A., Dash, J., Tompkins, E.L., Tonon, T., 2020. A systematic review of floating and beach landing records of *Sargassum* beyond the Sargasso Sea. Environ. Res. Commun. 2 (12), 122001. http://dx.doi.org/10.1088/2515-7620/abd109, URL: https://iopscience.iop.org/article/10.1088/2515-7620/abd109.

Gobert, T., Gautier, A., Connan, S., Rouget, M.-L., Thibaut, T., Stiger-Pouvreau, V., Waeles, M., 2022. Trace metal content from holopelagic *Sargassum* spp. sampled in the tropical North Atlantic Ocean: Emphasis on spatial variation of arsenic and phosphorus. Chemosphere 308, 136186. http://dx.doi.org/10.1016/j.chemosphere.2022.136186, URL: https://linkinghub.elsevier.com/retrieve/pii/S0045653522026790.

Grossowicz, M., Marques, G.M., Van Voorn, G.A., 2017. A dynamic energy budget (DEB) model to describe population dynamics of the marine cyanobacterium *Prochlorococcus marinus*. Ecol. Model. 359, 320–332. http://dx.doi.org/10.1016/j.ecolmodel.2017.06.011, URL: https://linkinghub.elsevier.com/retrieve/pii/S0304380017301473.

Guillaume, J.H., Jakeman, J.D., Marsili-Libelli, S., Asher, M., Brunner, P., Croke, B., Hill, M.C., Jakeman, A.J., Keesman, K.J., Razavi, S., Stigter, J.D., 2019. Introductory overview of identifiability analysis: A guide to evaluating whether you have the right type of data for your modeling purpose. Environ. Model. Softw. 119, 418–432. http://dx.doi.org/10.1016/j.envsoft.2019.07.007, URL: https://linkinghub.elsevier.com/retrieve/pii/S1364815218307278.

Hanisak, M.D., Samuel, M.A., 1987. Growth rates in culture of several species of *Sargassum* from Florida, USA. Hydrobiologia 151–152 (1), 399–404. http://dx.doi.org/10.1007/BF00046159, URL: http://link.springer.com/10.1007/BF00046159.

Hatt, D.C., Bally, N.K., Iporac, L.A.R., Olszak, S., Campbell, J.E., Collado-Vides, L., 2024. Comprehensive Analysis of Biomass, Nutrient, and Heavy Metal Contributions of Pelagic *Sargassum* Species (Phaeophyceae) Inundations in South Florida. Phycology 4 (2), 235–255. http://dx.doi.org/10.3390/phycology4020013, URL: https://www.mdpi.com/2673-9410/4/2/13.

Hatt, D.C., Nauer, F., Collado-Vides, L., Campbell, J.E., 2025. Physiological Responses of Pelagic *Sargassum* (Phaeophyceae) to Thermal Stress Vary by Species and Morphotype. Appl. Phycol. 6 (1), 1–19. http://dx.doi.org/10.1080/26388081.2025.2515422, URL: https://www.tandfonline.com/doi/full/10.1080/26388081.2025.2515422.

Jakeman, A.J., Elsawah, S., Wang, H.-H., Hamilton, S.H., Melsen, L., Grimm, V., 2024. Towards normalizing good practice across the whole modeling cycle: its instrumentation and future research topics. Socio-Environmental Syst. Model. 6, 18755. http://dx.doi.org/10.18174/sesmo.18755, URL: https://sesmo.org/article/view/18755.

Jouanno, J., Benshila, R., Berline, L., Soulié, A., Radenac, M.-H., Morvan, G., Diaz, F., Sheinbaum, J., Chevalier, C., Thibaut, T., Changeux, T., Menard, F., Berthet, S., Aumont, O., Ethé, C., Nabat, P., Mallet, M., 2021. A NEMO-based model of *Sargassum* distribution in the tropical Atlantic: description of the model and sensitivity analysis (NEMO-Sarg1.0). Geosci. Model. Dev. 14 (6), 4069–4086. http://dx.doi.org/10.5194/gmd-14-4069-2021, URL: https://gmd.copernicus.org/articles/14/4069/2021/.

Jouanno, J., Berthet, S., Muller-Karger, F., Aumont, O., Sheinbaum, J., 2025. An extreme North Atlantic Oscillation event drove the pelagic *Sargassum* tipping point. Commun. Earth Environ. 6 (1), 95. http://dx.doi.org/10.1038/s43247-025-02074-x, URL: https://www.nature.com/articles/s43247-025-02074-x.

Jusup, M., Sousa, T., Domingos, T., Labinac, V., Marn, N., Wang, Z., Klanjšˇcek, T., 2017. Physics of metabolic organization. Phys. Life Rev. 20, 1–39. http://dx.doi.org/10.1016/j.plrev.2016.09.001, URL: https://linkinghub.elsevier.com/retrieve/pii/S1571064516300902.

Kearney, M.R., Jusup, M., McGeoch, M.A., Kooijman, S.A.L.M., Chown, S.L., 2021. Where do functional traits come from? The role of theory and models. Funct. Ecol. 35 (7), 1385–1396. http://dx.doi.org/10.1111/1365-2435.13829, URL: https://besjournals.onlinelibrary.wiley.com/doi/10.1111/1365-2435.13829.

Kooijman, S., 1998. The Synthesizing Unit as model for the stoichiometric fusion and branching of metabolic fluxes. Biophys. Chem. 73 (1–2), 179–188. http://dx.doi.org/10.1016/S0301-4622(98)00162-8, URL: https://linkinghub.elsevier.com/retrieve/pii/S0301462298001628.

Kooijman, B., 2010. Dynamic Energy Budget Theory for Metabolic Organisation, third ed. Cambridge University Press, http://dx.doi.org/10.1017/CBO9780511805400, URL: https://www.cambridge.org/core/product/identifier/9780511805400/type/book.

Kooijman, S.A.L.M., Kearney, M.R., Marn, N., Sousa, T., Domingos, T., Lavaud, R., Récapet, C., Klanjšˇcek, T., Yeuw, T.T., Marques, G.M., Pecquerie, L., Lika, K., 2024. From formulae, via models to theories: Dynamic Energy Budget theory illustrates requirements. Ecol. Model. 497, 110869. http://dx.doi.org/10.1016/j.ecolmodel.2024.110869.

Kumar, S., Sahoo, D., Levine, I., 2015. Assessment of nutritional value in a brown seaweed *Sargassum wightii* and their seasonal variations. Algal Res. 9, 117–125. http://dx.doi.org/10.1016/j.algal.2015.02.024, URL: https://linkinghub.elsevier.com/retrieve/pii/S2211926415000508.

Lagunes, M.-J., Pecquerie, L., 2025. Supplementary Github: SargaDEB_SFF_NeededExperiments. http://dx.doi.org/10.5281/zenodo.17633290, https://zenodo.org/doi/10.5281/zenodo.17633290.

Lam, N.N., Docherty, P.D., Murray, R., 2022. Practical identifiability of parametrised models: A review of benefits and limitations of various approaches. Math. Comput. Simulation 199, 202–216. http://dx.doi.org/10.1016/j.matcom.2022.03.020, URL: https://linkinghub.elsevier.com/retrieve/pii/S0378475422001227.

Lapointe, B.E., 1986. Phosphorus-limited photosynthesis and growth of *Sargassum natans* and *Sargassum fluitans* (Phaeophyceae) in the western North Atlantic. Deep. Sea Res. Part A. Ocean. Res. Pap. 33 (3), 391–399. http://dx.doi.org/10.1016/0198-0149(86)90099-3, URL: https://linkinghub.elsevier.com/retrieve/pii/0198014986900993.

Lapointe, B.E., 1995. A comparison of nutrient-limited productivity in *Sargassum natans* from neritic vs. oceanic waters of the western North Atlantic Ocean. Limnol. Oceanogr. 40 (3), 625–633. http://dx.doi.org/10.4319/lo.1995.40.3.0625, URL: http://doi.wiley.com/10.4319/lo.1995.40.3.0625.

Lapointe, B.E., Brewton, R.A., Herren, L.W., Wang, M., Hu, C., McGillicuddy, D.J., Lindell, S., Hernandez, F.J., Morton, P.L., 2021. Nutrient content and stoichiometry of pelagic *Sargassum* reflects increasing nitrogen availability in the Atlantic Basin. Nat. Commun. 12 (1), 3060. http://dx.doi.org/10.1038/s41467-021-23135-7, URL: https://www.nature.com/articles/s41467-021-23135-7.

Lavaud, R., Filgueira, R., Nadeau, A., Steeves, L., Guyondet, T., 2020. A Dynamic Energy Budget model for the macroalga *Ulva lactuca* . Ecol. Model. 418, 108922. http://dx.doi.org/10.1016/j.ecolmodel.2019.108922, URL: https://linkinghub.elsevier.com/retrieve/pii/S0304380019304302.

Leemans, L., Magaña-Gallegos, E., Van Katwijk, M.M., Lamers, L.P., Smolders, A.J., Bouma, T.J., Christianen, M.J., Van Tussenbroek, B.I., 2025. Iron co-limitation of *Sargassum fluitans*. Aquat. Bot. 196, 103807. http://dx.doi.org/10.1016/j.aquabot.2024.103807, URL: https://linkinghub.elsevier.com/retrieve/pii/S0304377024000597.

Lika, K., Kearney, M.R., Freitas, V., Van Der Veer, H.W., Van Der Meer, J., Wijsman, J.W., Pecquerie, L., Kooijman, S.A., 2011. The "covariation method" for estimating the parameters of the standard Dynamic Energy Budget model I: Philosophy and approach. J. Sea Res. 66 (4), 270–277. http://dx.doi.org/10.1016/j.seares.2011.07.010, URL: https://linkinghub.elsevier.com/retrieve/pii/S1385110111001055.

Lika, K., Kooijman, S.A., 2024. The relationship between confidence intervals and distributions of estimators for parameters of deterministic models. Ecol. Model. 490, 110645. http://dx.doi.org/10.1016/j.ecolmodel.2024.110645, URL: https://linkinghub.elsevier.com/retrieve/pii/S0304380024000346.

Lika, K., Papadakis, I., 2009. Modeling the biodegradation of phenolic compounds by microalgae. J. Sea Res. 62 (2–3), 135–146. http://dx.doi.org/10.1016/j.seares.2009.02.005, URL: https://linkinghub.elsevier.com/retrieve/pii/S1385110109000252.

Livanou, E., Lagaria, A., Psarra, S., Lika, K., 2019. A DEB-based approach of modeling dissolved organic matter release by phytoplankton. J. Sea Res. 143, 140–151. http://dx.doi.org/10.1016/j.seares.2018.07.016, URL: https://linkinghub.elsevier.com/retrieve/pii/S1385110118300303.

Lorena, A., Marques, G.M., Kooijman, S.A.L.M., Sousa, T., 2010. Stylized facts in microalgal growth: interpretation in a dynamic energy budget context. Phil. Trans. R. Soc. B 365 (1557), 3509–3521. http://dx.doi.org/10.1098/rstb.2010.0101, URL: https://royalsocietypublishing.org/doi/10.1098/rstb.2010.0101.

Machado, C.B., Maddix, G.-M., Francis, P., Thomas, S.-L., Burton, J.-A., Langer, S., Larson, T.R., Marsh, R., Webber, M., Tonon, T., 2022. Pelagic *Sargassum* events in Jamaica: Provenance, morphotype abundance, and influence of sample processing on biochemical composition of the biomass. Sci. Total Environ. 817, 152761. http://dx.doi.org/10.1016/j.scitotenv.2021.152761, URL: https://linkinghub.elsevier.com/retrieve/pii/S0048969721078402.

Magaña-Gallegos, E., García-Sánchez, M., Graham, C., Olivos-Ortiz, A., Siuda, A.N., Van Tussenbroek, B.I., 2023a. Growth rates of pelagic *Sargassum* species in the Mexican Caribbean. Aquat. Bot. 185, 103614. http://dx.doi.org/10.1016/j.aquabot.2022.103614, URL: https://linkinghub.elsevier.com/retrieve/pii/S0304377022001267.

Magaña-Gallegos, E., Villegas-Muñoz, E., Salas-Acosta, E.R., Barba-Santos, M.G., Silva, R., Van Tussenbroek, B.I., 2023b. The Effect of temperature on the growth of holopelagic *Sargassum* species. Phycology 3 (1), 138–146. http://dx.doi.org/10.3390/phycology3010009, URL: https://www.mdpi.com/2673-9410/3/1/9.

Marques, G.M., Augustine, S., Lika, K., Pecquerie, L., Domingos, T., Kooijman, S.A.L.M., 2018. The AmP project: Comparing species on the basis of dynamic energy budget parameters. In: Beard, D.A. (Ed.), PLoS Comput. Biol. 14 (5), e1006100. http://dx.doi.org/10.1371/journal.pcbi.1006100, URL: https://dx.plos.org/10.1371/journal.pcbi.1006100.

Marques, G.M., Lika, K., Augustine, S., Pecquerie, L., Kooijman, S.A., 2019. Fitting multiple models to multiple data sets. J. Sea Res. 143, 48–56. http://dx.doi.org/10.1016/j.seares.2018.07.004, URL: https://linkinghub.elsevier.com/retrieve/pii/S1385110117303441.

Marsh, R., Addo, K.A., Jayson-Quashigah, P.-N., Oxenford, H.A., Maxam, A., Anderson, R., Skliris, N., Dash, J., Tompkins, E.L., 2021. Seasonal Predictions of Holopelagic *Sargassum* Across the Tropical Atlantic Accounting for Uncertainty in Drivers and Processes: The SARTRAC Ensemble Forecast System. Front. Mar. Sci. 8, 722524. http://dx.doi.org/10.3389/fmars.2021.722524, URL: https://www.frontiersin.org/articles/10.3389/fmars.2021.722524/full.

Marsh, R., Oxenford, H.A., Cox, S.-A.L., Johnson, D.R., Bellamy, J., 2022. Forecasting seasonal sargassum events across the tropical Atlantic: Overview and challenges. Front. Mar. Sci. 9, 914501. http://dx.doi.org/10.3389/fmars.2022.914501, URL: https://www.frontiersin.org/articles/10.3389/fmars.2022.914501/full.

Meer, J.v.d., 2006. An introduction to Dynamic Energy Budget (DEB) models with special emphasis on parameter estimation. J. Sea Res. 56, 85–102. http://dx.doi.org/10.1016/j.seares.2006.03.001.

Monaco, C.J., Porporato, E.M.D., Lathlean, J.A., Tagliarolo, M., Sara, G., 2019. Predicting the performance of cosmopolitan species: dynamic energy budget model skill drops across large spatial scales. Mar. Biol. 166, 14. http://dx.doi.org/10.1007/s00227-018-3462-4.

Nisbet, R.M., Jusup, M., Klanjscek, T., Pecquerie, L., 2012. Integrating dynamic energy budget (DEB) theory with traditional bioenergetic models. J. Exp. Biol. 215 (6), 892–902. http://dx.doi.org/10.1242/jeb.059675, URL: https://journals.biologists.com/jeb/article/215/6/892/11211/Integrating-dynamic-energy-budget-DEB-theory-with.

Oliveira, D.F., Marques, G.M., Carolino, N., Pais, J., Sousa, J.M.C., Domingos, T., 2024. A multi-tier methodology for the estimation of individual-specific parameters of DEB models. Ecol. Model. 494, 110779. http://dx.doi.org/10.1016/j.ecolmodel.2024.110779, URL: https://www.sciencedirect.com/science/article/pii/S0304380024001674.

Papadakis, I., Kotzabasis, K., Lika, K., 2005. A cell-based model for the photoacclimation and CO2-acclimation of the photosynthetic apparatus. Biochim. et Biophys. Acta (BBA) - Bioenerg. 1708 (2), 250–261. http://dx.doi.org/10.1016/j.bbabio.2005.03.001, URL: https://linkinghub.elsevier.com/retrieve/pii/S0005272805000836.

Payne, K., Greene, K., Oxenford, H.A., 2024. A Parallelized Climatological Drifter-Based Model of Sargassum Biomass Dynamics in the Tropical Atlantic. J. Mar. Sci. Eng. 12 (7), 1214. http://dx.doi.org/10.3390/jmse12071214, URL: https://www.mdpi.com/2077-1312/12/7/1214.

Podlejski, W., Berline, L., Jouanno, J., Barrier, N., Lett, C., 2024. Drivers of growth and decay of Sargassum in the Tropical Atlantic: A Lagrangian approach. Prog. Oceanogr. 229, 103364. http://dx.doi.org/10.1016/j.pocean.2024.103364, URL: https://linkinghub.elsevier.com/retrieve/pii/S0079661124001708.

Poggiale, J.-C., Baklouti, M., Queguiner, B., Kooijman, S.A.L.M., 2010. How far details are important in ecosystem modelling: the case of multi-limiting nutrients in phytoplankton–zooplankton interactions. Phil. Trans. R. Soc. B 365 (1557), 3495–3507. http://dx.doi.org/10.1098/rstb.2010.0165, URL: https://royalsocietypublishing.org/doi/10.1098/rstb.2010.0165.

Putman, N.F., Lumpkin, R., Olascoaga, M.J., Trinanes, J., Goni, G.J., 2020. Improving transport predictions of pelagic *Sargassum*. J. Exp. Mar. Biol. Ecol. 529, 151398. http://dx.doi.org/10.1016/j.jembe.2020.151398, URL: https://linkinghub.elsevier.com/retrieve/pii/S0022098120300125.

Raue, A., Becker, V., Klingmüller, U., Timmer, J., 2010. Identifiability and observability analysis for experimental design in nonlinear dynamical models. Chaos: An Interdiscip. J. Nonlinear Sci. 20 (4), 045105. http://dx.doi.org/10.1063/1.3528102, URL: https://pubs.aip.org/cha/article/20/4/045105/152044/Identifiability-and-observability-analysis-for.

Schell, J., Goodwin, D., Siuda, A., 2015. Recent *Sargassum* Inundation Events in the Caribbean: Shipboard Observations Reveal Dominance of a Previously Rare Form. Oceanography 28 (3), 8–10. http://dx.doi.org/10.5670/oceanog.2015.70, URL: https://tos.org/oceanography/article/recent-sargassum-inundation-events-in-the-caribbean-shipboard-observations.

Schell, J.M., Goodwin, D.S., Volk, R.H., Siuda, A.N., 2024. Preliminary explorations of environmental tolerances and growth rates of holopelagic *Sargassum* morphotypes. Aquat. Bot. 190, 103723. http://dx.doi.org/10.1016/j.aquabot.2023.103723, URL: https://linkinghub.elsevier.com/retrieve/pii/S0304377023001080.

Schoolfield, R., Sharpe, P., Magnuson, C., 1981. Non-linear regression of biological temperature-dependent rate models based on absolute reaction-rate theory. J. Theoret. Biol. 88 (4), 719–731. http://dx.doi.org/10.1016/0022-5193(81)90246-0, URL: https://linkinghub.elsevier.com/retrieve/pii/0022519381902460.

Sellner, K.G., Doucette, G.J., Kirkpatrick, G.J., 2003. Harmful algal blooms: causes, impacts and detection. J. Ind. Microbiol. Biotechnol. 30 (7), 383–406. http://dx.doi.org/10.1007/s10295-003-0074-9, URL: https://academic.oup.com/jimb/article/30/7/383/5992140.

Siuda, A.N.S., Blanfuné, A., Dibner, S., Verlaque, M., Boudouresque, C.-F., Connan, S., Goodwin, D.S., Stiger-Pouvreau, V., Viard, F., Rousseau, F., Michotey, V., Schell, J.M., Changeaux, T., Aurelle, D., Thibaut, T., 2024. Morphological and Molecular Characters Differentiate Common Morphotypes of Atlantic Holopelagic *Sargassum*. Phycology 4 (2), 256–275. http://dx.doi.org/10.3390/phycology4020014, URL: https://www.mdpi.com/2673-9410/4/2/14.

Sousa, T., Domingos, T., Poggiale, J.-C., Kooijman, S.A.L.M., 2010. Dynamic energy budget theory restores coherence in biology. Phil. Trans. R. Soc. B 365 (1557), 3413–3428. http://dx.doi.org/10.1098/rstb.2010.0166, URL: https://royalsocietypublishing.org/doi/10.1098/rstb.2010.0166.

Sun, K., Ruan, S., Zhang, X., Xu, D., Fan, X., Wang, Y., Wang, W., Zhang, P., Wang, L., Ye, N., 2026. Modelling the winter Sargassum blooms in the Yellow Sea: considering wind, current and growth. Ecol. Model. 511, 111387. http://dx.doi.org/10.1016/j.ecolmodel.2025.111387, URL: https://linkinghub.elsevier.com/retrieve/pii/S0304380025003734.

Tonon, T., Machado, C.B., Webber, M., Webber, D., Smith, J., Pilsbury, A., Cicéron, F., Herrera-Rodriguez, L., Jimenez, E.M., Suarez, J.V., Ahearn, M., Gonzalez, F., Allen, M.J., 2022. Biochemical and Elemental Composition of Pelagic *Sargassum* Biomass Harvested across the Caribbean. Phycology 2 (1), 204–215. http://dx.doi.org/10.3390/phycology2010011, URL: https://www.mdpi.com/2673-9410/2/1/11.

Vásquez-Elizondo, R.M., Vázquez-Delfín, E., Robledo, D., 2023. Growth and photosynthetic physiology of holopelagic *Sargassum* (Phaeophyceae) under laboratory conditions. Phycol. Res. pre.12541. http://dx.doi.org/10.1111/pre.12541, URL: https://onlinelibrary.wiley.com/doi/10.1111/pre.12541.

Venolia, C.T., Lavaud, R., Green-Gavrielidis, L.A., Thornber, C., Humphries, A.T., 2020. Modeling the Growth of Sugar Kelp (*Saccharina latissima*) in Aquaculture Systems using Dynamic Energy Budget Theory. Ecol. Model. 430, 109151. http://dx.doi.org/10.1016/j.ecolmodel.2020.109151, URL: https://linkinghub.elsevier.com/retrieve/pii/S0304380020302222.

Wang, M., Hu, C., Barnes, B.B., Mitchum, G., Lapointe, B., Montoya, J.P., 2019. The great Atlantic *Sargassum* belt. Science 365 (6448), 83–87. http://dx.doi.org/10.1126/science.aaw7912, URL: https://www.science.org/doi/10.1126/science.aaw7912.

Wieland, F.-G., Hauber, A.L., Rosenblatt, M., Tönsing, C., Timmer, J., 2021. On structural and practical identifiability. Curr. Opin. Syst. Biol. 25, 60–69. http://dx.doi.org/10.1016/j.coisb.2021.03.005, Publisher: Elsevier BV, URL: https://linkinghub.elsevier.com/retrieve/pii/S245231002100007X.

Winarni, S., Zainuri, M., Endrawati, H., Arifan, F., Setyawan, A., Wangi, A.P., 2021. Analysis proximate of sargassum seaweed sp. J. Phys.: Conf. Ser. 1943 (1), 012173. http://dx.doi.org/10.1088/1742-6596/1943/1/012173, URL: https://iopscience.iop.org/article/10.1088/1742-6596/1943/1/012173.

Zurell, D., Berger, U., Cabral, J.S., Jeltsch, F., Meynard, C.N., Münkemüller, T., Nehrbass, N., Pagel, J., Reineking, B., Schröder, B., Grimm, V., 2010. The virtual ecologist approach: simulating data and observers. Oikos 119 (4), 622–635. http://dx.doi.org/10.1111/j.1600-0706.2009.18284.x, URL: https://nsojournals.onlinelibrary.wiley.com/doi/10.1111/j.1600-0706.2009.18284.x.